Optimization of Radially Heterogeneous 1000-MW(e) LMFBR Core Configurations

Volume 4: Appendixes D and E

EPRI

EPRI NP-1000
Volume 4
Project 620-25
Interim Report
November 1979

Keywords:
LMFBR Core
HCDA
Heterogeneous Core
No Void Coefficient
Bull's-Eye Core

Prepared by
Argonne National Laboratory
Argonne, Illinois

ELECTRIC POWER RESEARCH INSTITUTE

Optimization of Radially Heterogeneous 1000-MW(e) LMFBR Core Configurations
Volume 4: Appendixes D and E

NP-1000, Volume 4
Research Project 620-25

Interim Report, November 1979

Prepared by

ARGONNE NATIONAL LABORATORY
Applied Physics Division
EBR-II Division
9700 South Cass Avenue
Argonne, Illinois 60439

Principal Investigators
W. P. Barthold
Y. Orechwa
S. F. Su
E. Hutter
R. V. Batch
J. C. Beitel
R. B. Turski
P. S. K. Lam

Prepared for

Electric Power Research Institute
3412 Hillview Avenue
Palo Alto, California 94304

EPRI Project Manager
Edward L. Fuller
Nuclear Power Division

ORDERING INFORMATION

Requests for copies of this report should be directed to Research Reports Center (RRC), Box 50490, Palo Alto, CA 94303 (415) 961-9043 There is no charge for reports requested by EPRI member utilities and affiliates contributing nonmembers, U S utility associations, U S government agencies (federal, state, and local), media and foreign organizations with which EPRI has an information exchange agreement On request, RRC will send a catalog of EPRI reports

NOTICE

This report was prepared by the organization(s) named below as an account of work sponsored by the Electric Power Research Institute Inc (EPRI) Neither EPRI members of EPRI the organization(s) named below nor any person acting on their behalf (a) makes any warranty or representation express or implied with respect to the accuracy completeness or usefulness of the information contained in this report or that the use of any information apparatus method or process disclosed in this report may not infringe privately owned rights or (b) assumes any liabilities with respect to the use of or for damages resulting from the use of any information apparatus method or process disclosed in this report

Prepared by
Argonne National Laboratory
Argonne, Illinois

DISCLAIMER

EPRI PERSPECTIVE

PROJECT DESCRIPTION

A hypothetical core disruptive accident (HCDA) and the impact it might cause, particularly on the underside of the head of a liquid metal fast breeder reactor (LMFBR) is a controversial issue. The debate is how much capability for safe absorption of impact energy must be designed into the reactor vessel and head. Neutronics and thermo-hydraulics analysts and core designers are the ones to whom this report is directed. Reactor vendors of early large-size LMFBRs can use this work as a sound starting base for improvements. The immediate application of this work is to provide the core design for the prototype large breeder reactor design studies conducted under EPRI Research Project 620.

This work, "Optimization of Radially Heterogeneous 1000-MW(e) LMFBR Core Configurations," is presented in four volumes. These are as follows:

- Volume 1: Design and Performance of Reference Cores
- Volume 2: Appendix A--Design Assumptions and Constraints
  Appendix B--Radially Heterogeneous Core Configurations
- Volume 3: Appendix C--Optimization of Core Performance Parameters
- Volume 4: Appendix D--Optimization of Core Configurations
  Appendix E--Component Designs

PROJECT OBJECTIVES

The objective of the work reported here is to make the characteristics of large cores such that the impact energy of an HCDA would approach zero. Without special provisions, an LMFBR vessel and head will have greater impact resistance than would be needed by such a core, thus relieving the controversy and assuring a safe design feature.

This report presents the results of the second of three phases of effort to optimize a radial heterogeneous 1000-MW(e) LMFBR core design that will minimize energetics in

an HCDA and yet have highly desirable breeding gain and core performance. The final results of the three phases are intended to establish a reference core design that will be safe, licensable, reliable, and efficient.

PROJECT RESULTS

Although not reflected in the work reported, doubling time is not the simple figure of merit that it originally appeared to be. A minimum compound system doubling time is quite desirable when the U.S. utility industry is plutonium limited, i.e., all of the available Pu (owned by the utilities) is being fully utilized in breeder plants. However, this is not the case and probably will not be true until well after the year 2010. Emphasis will be shifted to maximize total net plutonium produced rather than doubling time. In-core inventory will optimize at a somewhat higher quantity of Pu.

As stated in the text there are too many uncertainties in the fuel costs to make them a figure of merit between designs. However, on a consistent basis of estimating, the promising core designs show only small differences in costs. It is highly probable that costs can be significantly improved over those listed in the text.

Edward L. Fuller, Project Manager
R. K. Winkleblack, Program Manager
Nuclear Power Division

ABSTRACT

A parameter study was conducted to determine the interrelated effects of: loosely or tightly coupled fuel regions separated by internal blanket assemblies, number of fuel regions, core height, number and arrangement of internal blanket subassemblies, number and size of fuel pins in a subassembly, etc. The effects of these parameters on sodium void reactivity, Doppler, "incoherence," breeding gain, and thermohydraulics were of prime interest. Trends were established and ground work laid for optimization of a large, radially-heterogeneous, LMFBR core that will have low energetics in an HCDA and will have good thermal and breeding performance.

APPENDIX D: OPTIMIZATION OF CORE CONFIGURATIONS

Table of Contents

		Page
1.0	INTRODUCTION	D-1
2.0	APPROACH	D-3
3.0	CONFIGURATIONS	D-5
	3.1 40 IN. CORE HEIGHT	D-5
	3.2 36 IN. CORE HEIGHT	D-8
4.0	PERFORMANCE CHARACTERISTICS	D-9
	4.1 INVENTORY	D-9
	4.2 BURNUP AND BURNUP SWING	D-10
	4.3 FAST FLUENCE	D-10
	4.4 POWER SWING	D-11
	4.5 POWER SHAPE SENSITIVITY	D-11
	4.6 BREEDING	D-12
	4.7 SODIUM VOID REACTIVITY	D-13
5.0	SELECTION OF MOST PROMISING CONFIGURATIONS	D-15
	5.1 40 IN. HIGH CORES	D-15
	5.2 36 IN. HIGH CORES	D-17
6.0	SUMMARY AND CONCLUSIONS	D-19

List of Figures

No.	Title	Page
1.	Layout for 40 in. Core - Reference Configuration	D-22
2.	Layout for 40 in. Core - Configuration 1	D-22
3.	Layout for 40 in. Core - Configuration 2	D-23
4.	Layout for 40 in. Core - Configuration 3	D-23
5.	Layout for 40 in. Core - Configuration 4	D-24
6.	Layout for 40 in. Core - Configuration 5	D-24
7.	Layout for 40 in. Core - Configuration 6	D-25
8.	Layout for 40 in. Core - Configuration 7	D-25
9.	Layout for 40 in. Core - Configuration 8	D-26
10.	Layout for 40 in. Core - Configuration 9	D-26
11.	Layout for 40 in. Core - Configuration 10	D-27
12.	Layout for 40 in. Core - Configuration 11	D-27
13.	Layout for 40 in. Core - Configuration 12a	D-28
14.	Layout for 40 in. Core - Configuration 12b	D-28
15.	Layout for 40 in. Core - Configuration 12c	D-29
16.	Layout for 36 in. Core - Reference Configuration	D-29
17.	Layout for 36 in. Core - Configuration 1	D-30
18.	Layout for 36 in. Core - Configuration 2	D-30
19.	Layout for 36 in. Core - Configuration 3	D-31
20.	Layout for 36 in. Core - Configuration 4	D-31
21.	Layout for 36 in. Core - Configuration 5	D-32
22.	BOEC Assembly-Wise Peak Power Density for Configuration 12a 40 in. Core	D-32
23.	BOEC Assembly-Wise Peak Power Density for Configuration 12b 40 in. Core	D-33
24.	BOEC Assembly-Wise Peak Power Density for Configuration 12c 40 in. Core	D-34
25.	EOEC Assembly-Wise Peak Power Density for Configuration 12a 40 in. Core	D-35
26.	EOEC Assembly-Wise Peak Power Density for Configuration 12b 40 in. Core	D-36
27.	EOEC Assembly-Wise Peak Power Density for Configuration 12c 40 in. Core	D-37

No.	Title	Page
28.	BOL Assembly-Wise Peak Power Density for Reference 36 in. Core - All Rods Out	D-38
29.	BOL Assembly-Wise Peak Power Density for Reference 36 in. Core - Row 11 Rods In	D-39
30.	BOL Assembly-Wise Peak Power Density for Configuration 5 36 in. Core - All Rods Out	D-40
31.	BOL Assembly-Wise Peak Power Density for Configuration 5 36 in. Core - Row 11 Rods In	D-41

List of Tables

No.	Title	Page
I.	Number of Assemblies per Region for 40 in. Cores	D-42
II.	Number of Assemblies per Region for 36 in. Cores	D-43
III.	Inventory for 40 in. Cores	D-44
IV.	Inventories for 36 in. Cores	D-45
V.	Burnup Parameters for 40 in. Cores	D-46
VI.	Burnup Parameters for 36 in. Cores	D-46
VII.	Rating, Power Swings and Power Sensitivities to Enrichment Split Changes for 40 in. Cores	D-47
VIII.	Rating, Power Swings and Power Sensitivities to Enrichment Split Change for 36 in. Cores	D-48
IX.	Breeding Performances and Sodium Void Reactivities for 40 in. Cores	D-49
X.	Breeding Performances and Sodium Void Reactivities for 36 in. Cores	D-50
XI.	Peak-to-Average Ratings for 40 in. Core With 12a, 12b and 12c Core Configuration (HEX Calculations)	D-50
XII.	Peak Ratings (kW/ft) for 40 in. Cores With 12a, 12b and 12c Core Configurations (HEX Calculations)	D-51
XIII.	Control Rod Worths for 40 in. Cores With 12a, 12b and 12c Core Configurations	D-51

1.0 INTRODUCTION

The previous analyses reported in Appendix B showed that loosely coupled cores at a core height of 40 in. were capable of achieving sodium void reactivities in the \$2.00 - \$2.50 range. For tightly coupled cores, on the other hand, core heights of less than 40 in. were required to achieve similar sodium void reactivities. Consequently, in the subsequent analysis of core performance parameters reported in Appendix C loosely coupled cores were analyzed for 40 in. and 48 in. core heights, and tightly coupled cores for 32 in. and 36 in. core heights. The purpose of that subsequent analysis was to determine required core heights, identify optimum pin diameters, assess center core vs. center blanket configurations and ultimately select two promising basic core configurations on which improvements would then be made.

None of the systems analyzed in Appendix C which differed in number of core regions, neutronic coupling, core height and pin diameter was a clear favorite. However, because of the high power swing and high power peaking sensitivity to small enrichment changes observed for the center core configurations, they were eliminated from further analyses. The two basic core configurations selected for improvements, one loosely coupled and one tightly coupled, were both center blanket, three core zone arrangements. These arrangements were selected in preference over the two or four core region arrangements. They allowed for more flexibility in design modification than the two core region arrangements, which had very little margin for improvement. And yet they were not as complex in design as the four core region arrangements, which exhibited about equal performance characteristics in almost very aspect as the three core region arrangements.

The basic design characteristics of the two core selected for improvement were

Coupling	Configuration	Core Zones	Core Height	Fuel Pins Per Assembly	Fuel Pin Diameter
LC	CB	3	40	271	0.26 in.
TC	CB	3	36	331	0.24 in.

LC - loosely coupled, TC - tightly coupled, CB - center blanket

The 40 in. loosely coupled core had 271 pins per fuel assembly whereas the 36 in. tightly coupled core had 331. The 0.26 in. and 0.24 in. fuel pin diameters selected were the optimum pin diameters with respect to doubling time for the respective systems.

The purpose of this study was to, develop an optimum configuration for each of these systems by modifying the original core layouts while retaining the above design parameters. The selection of the final core design for conceptual design would then be made after more detailed nuclear, thermal-hydraulic and mechanical design analyses.

2.0 APPROACH

For the optimization of the configurations, the fuel pin diameters for the core height of 40 in. and 36 in. were kept at 0.26 in. and 0.24 in. respectively, because the optimum fuel pin diameter is primarily determined by the core height and is affected little by modifications in core configuration. The design of the fuel assemblies was constrained by a p/d ratio of 1.18 and a fuel bundle pressure drop of 75 psi. For the particular combinations of core height and pin diameter, i.e. a 40 in. core with 0.26 in. pins and a 36 in. core with 0.24 in. pins, the pressure drop constraint limited the design. For each core height and pin diameter, clad thickness, axial blanket thickness and plenum length were adjusted. The fuel cladding thickness to diameter ratio was kept constant at 0.050. The fuel to plenum length ratio was kept at 1.0. The 40 in. core had 15 in. axial blankets. For the 36 in. core, they were increased to 16 in. to account for enhanced axial neutron leakage. The number of pins per fuel assembly for the original designs was adopted so that the assembly size remained in the neighborhood of 5.5 in.

The fuel and internal blanket residence time was fixed to two years. The radial blanket assemblies stayed in the reactor for five years. The reactor was refueled annually with 255.5 full power days per year, equivalent to a 70% load factor. The equilibrium cycle burnup analysis was conducted in r-z geometry.

The optimization of the core configuration was constrained by the $2.50 sodium void reactivity limit. Only configurations which were able to meet this limit were analyzed in more detail. Among those configurations, the major criteria for the optimization were (1) the sensitivity of the power shape to slight changes in enrichment split and (2) the maximum power swing in a fuel assembly over a burnup cycle. Specific inventory, doubling time and burnup swing were also considered in this optimization process but these figures of merit are less important for the selection process than power shape sensitivity and power swing.

When all the above criteria failed to distinctively distinguish one configuration from another, assessments were then made with respect to power peaking performance and control simplicity. To this end the analysis was carried out in hex geometry.

3.0 CONFIGURATIONS

The previous optimization analysis of core performance parameters reported in Appendix C had narrowed down the selection of optimum core designs to two candidates: a loosely-coupled 40 in. core with 0.26 in. fuel pin diameter and a tightly-coupled 36 in. core with 0.24 in. fuel pin diameter. Before the final selection was made, the core layouts of these two candidate cores were modified to see if any improvement could be made with regard to breeding performance, power peaking, power shape sensitivity, power swing, etc. The pin diameters for the respective cores remained unchanged during the optimization of the configuration. The modification for the 40 in. core concentrated on tightening the coupling and at the same time reducing the core region sizes to keep the sodium void reactivity below $2.50. The modifications for the 36 in. core emphasized the reduction of the center blanket size and the creation of a broken ring-arrangement of internal blanket assemblies to improve the power peaking performance and to simplify the reactivity control.

3.1 40 IN. CORE HEIGHT

Figure 1 shows the core layout of the original 40 in. loosely-coupled core described in Appendix C. The modified core configurations, designated as configurations 1-11 and 12a, 12b and 12c, which evolved from this reference configuration are shown in Figs. 2 to 15. All the modified configurations retained the basic center blanket, three core region arrangement of the reference configurations. They had 330 to 366 fuel assemblies and 133 to 181 internal blanket assemblies, as compared to 366 fuel and 181 internal blanket assemblies for the original design (Table I).

In the reference configuration, the internal blanket region that separated the first two core regions was close to one and a half rows thick and the one that separated the second and third core regions was slightly less than two rows thick. In the first modification (configuration 1), the core region size remained unchanged but the internal blanket rings were rearranged so that they became one or two full rows thick, respectively. This configuration offered no improvement with respect to power shape sensitivity to small enrichment changes

and power swing, although it had a slightly higher sodium void reactivity than the reference configuration. (Quantitative discussions of these and other performance parameters are given in Section 4.0.) Consequently, in configuration 2, twenty-four blanket assemblies were removed from the outer internal blanket ring to tighten the coupling between the two outer core regions. This configuration, as it turned out, resulted in only minor improvements in power shape sensitivity and power swing, despite a substantial increase in the sodium void reactivity.

Configurations 3 and 4 both employed a broken internal blanket ring to decouple the first and second core regions. The outer internal blanket ring occupied two full rows in configuration 3 and had 18 fewer assemblies in configuration 4. The sizes of the first and third core regions in both configurations were identical to those in configuration 2, but their second core region was 6 assemblies smaller. Configuration 4 had lower power shape sensitivity and power swing than all previous core layouts. Unfortunately, its sodium void reactivity exceeded the $2.50 limit. The size of the outermost core region was reduced by 18 assemblies in the next modification (configuration 5), bring the total number of fuel assemblies down to 342.

Configuration 6, 7, and 8 had also 342 fuel assemblies. However, they had fewer fuel assemblies in the first two core regions and more in the third than configuration 5. The three configurations differed in blanket arrangement, but the size of the individual core region and the total number of fuel and/or blanket assemblies were kept the same.

All these three configurations achieved practically the same sodium void reactivity (slightly below $2.50) as configuration 5 even though they had 12 fewer internal blanket assemblies. In terms of sodium void reduction, this indicated a better split between the core region sizes was used in these configurations than in configuration 5. In the modifications that followed, this new core region size split was adopted. Specifically, an arrangement of the first two core regions identical to configuration 8 was chosen because it provided the tightest coupling between the first two core regions due to the broken ring arrangement. Furthermore, with the broken ring arrangement power peaks were created. Placing control rods near the peak power locations not only increased the worth of the control rods but also provided a more uniform power shape control than in a closed-ring arrangement.

With configuration 8, a relatively low power shape sensitivity to enrichment variations was achieved. However, no significant improvement in power

swing was observed. The sodium void reactivity was only marginally below $2.50. More modifications were in order.

Configurations 9 and 10 had 12 more internal blanket assemblies than configuration 8. In configuration 9 these additional blanket assemblies were placed in the outermost internal blanket region. In configuration 10 they were placed in the third core region as isolated assemblies. A greater reduction in sodium void reactivity was obtained with the former. However, a significantly lower power swing was observed for the latter, due to the presence of the isolated internal blanket assemblies which enhanced the internal breeding in the third core region. The latter configuration also showed a lower power shape sensitivity and a lower burnup swing.

With the above findings, the evolution from configuration 10 to configuration 11 involved moving 12 blanket assemblies away from the outer internal blanket ring and placing them into the third core region next to the isolated internal blanket assemblies. By doing so, not only the internal breeding in the third core region was further improved but also the coupling of this core region with the other core regions was tightened. As a result, this core had achieved an extremely low burnup and power swings and a very low power shape sensitivity, with respect to all the previous cores.

In configuration 12a, 12 fuel assemblies adjacent to the isolated blanket assemblies were replaced by internal blanket assemblies to reduce the sodium void reactivity, which slightly exceeded $2.50 for configuration 11. Only a negligible penalty incurred in the power shape sensitivity. The power and burnup swing were further reduced. This core had a total of 330 fuel assemblies and 157 internal blanket assemblies.

Configurations 12b and 12c were variations of 12a. The locations of the control rods in the first two core regions were different. The arrangement of the isolated internal blanket assemblies in the third core region was also slightly modified in configuration 12c. They were otherwise identical to configuration 12a. Based on r-z analyses, they had the same performance characteristics as configuration 12a. However, substantial differences were observed in terms of power peaking, peak rating, and control rod worth, etc., when the more detailed hexagonal geometry analyses were carried out.

3.2 36 IN. CORE HEIGHT

The reference 36 in. core described in Appendix C (see Fig. 16) had a 55-assembly center blanket region and two complete rings of internal blanket each exactly one row thick to separate three core regions. Since it was already a tightly-coupled system, the power swing and power shape sensitivity were both low. The modifications for this core (see configurations 1-5 in Figs. 17 to 21) concentrated on reducing the center-blanket size and on the creation of a broken-ring arrangement that would give a good power peaking performance. The coupling between core regions was changed very little. The power swing and power shape sensitivity to enrichment variations were therefore only slightly affected by the modifications.

The reference core had 354 fuel and 169 internal blanket assemblies. The modified cores had from 342 to 354 fuel assemblies and from 109 to 145 internal blanket assemblies (Table II).

The center blanket was first reduced to three full rows (19 assemblies) in configuration 1 and 2, where closed-ring arrangements were retained. However, for the subsequent modifications, the center blanket was increased to four rows (31 assemblies) because a three-row center blanket would result in unacceptably high sodium void reactivities unless a significant change in coupling between the core regions was incorporated.

Configurations 3 to 5 all used a broken ring arrangement. They had 30 control rod assemblies compared to 24 for the reference and the first two configurations. The arrangement of the second internal blanket region was identical for the three configurations. Configuration 4 had 12 more assemblies in the outer internal blanket ring than configuration 3 to bring the sodium void reactivity to below \$2.50. The control rods at the internal blanket openings were shifted one row inward in configuration 5 to improve the power peaking performance. The removal of 12 fuel assemblies from the outer edges of the third core region was for the same purpose.

4.0 PERFORMANCE CHARACTERISTIC

For the performance analysis reported in Appendix C, a reactor power of 3,000 MWt was assumed for both reference cores. The peak linear heat ratings were in the range of 10-11 kW/ft which is well below the allowable rating of 13.5 kW/ft. Therefore, for the performance analysis presented in this Appendix, the reactor power for these cores was raised by 10%. The corresponding average fuel pin ratings were approximately 9 kW/ft. The reactor power for the other cores was set directly proportional to the number of fuel assemblies of each core, with the exception of the two final core designs whose powers were further raised by 3%. For all calculations, the enrichments were selected such that for each core region the peak ratings during fuel life were the same. Unless specified otherwise, the performance data discussed below were based on r-z calculations.

4.1 INVENTORY

Equilibrium cycle inventories and specific inventories are listed in Tables III and IV for the 40 in. and 36 in. high cores. The BOEC inventories for the 40 in. high cores ranged from 4132.2 kg for configuration 8 to 4708.5 kg for the reference configuration. The large spread in inventory is attributed to the different reactor sizes as well as the differences in neutronic coupling. The specific inventory, had a much smaller variation, ranging from 1.34 to 1.43 kg/MWt.

The BOEC inventory for the 36 in. high cores was the lowest (4006.7 kg) for configuration 1 and the highest for the reference configuration (4400.8 kg). (Except for the large difference in the center-blanket size, these two cores were quite similar in that they both had two complete rings of internal blanket each exactly one row thick.) The corresponding specific inventories were 1.21 and 1.33 kg/MWt, respectively. As will be shown later, configuration 1 had a sodium void reactivity greatly exceeding the $2.50 limit. Except for this configuration, the specific inventories for all 36 in. cores analyzed fell into a very narrow range of 1.27 to 1.33 kg/MWt. The specific inventory, therefore, was not an important figure of merit in the optimization of the configuration for neither the 36 in. high cores nor the 40 in. high cores.

The 36 in. high cores generally had lower specific inventories than the 40 in. cores primarily because a small fuel pin size was used for the former (0.24 in. o.d. for 36 in. high cores and 0.26 in. o.d. for 40 in. high cores).

Table IV shows a special case that used 42 in. core height instead of 36 in. This core had the same core layout as configuration 5 but it had 271 instead of 331 fuel pins in the driver assemblies. The fuel pin o.d. was increased to 0.27 in. so that the same assembly size as the 36 in. core was retained. The specific inventory in this case was approximately 8% higher than the 36 in. core with the same core layout.

4.2 BURNUP AND BURNUP SWING

For all 40 in. and 36 in. cores the net fissile gain over an equilibrium cycle was approximately 300 kg (Tables III and IV). The gain in fissile material in the internal blanket assemblies for the 40 in. cores was 23.4 to 57.2 kg higher than the loss in the driver fuel assemblies. For the 36 in. cores, the loss in the driver fuel assemblies in some cases exceeded the gain in the internal blanket assemblies. The combined fissile gain for the radial and axial blanket regions varied from 249.3 kg to 279 kg for 40 in. cores and from 296.6 kg to 319.1 kg for 36 in. cores.

Tables V and VI list burnup parameters for the 40 in. and 36 in. cores. The burnup swing for the 40 in. cores ranged from 0.49% to 1.52%. The lowest burnup swings were seen for configurations 12a, b and c. The burnup swing was generally higher for the 36 in. cores, with the lowest being 1.49%. The special 42 in. core previously described had a burnup swing of 0.94%, i.e., 0.49% lower than the corresponding 36 in. core.

The peak discharge burnup for 40 in. showed only small variations with the configuration, ranging from 82.0 to 85.4 MWD/kg. The peak discharge burnups for 36 in. core were less uniform. They ranged from 83.3 to 92.9 MWD/kg. The generally higher burnups for 36 in. cores reflected the difference in driver fuel pin size.

4.3 FAST FLUENCE

The smaller fuel pin size for the 36 in. cores leads also to higher fluences for the 36 in. cores. Nevertheless, the fluences were all substantially lower than those seen in homogeneous cores with the same pin size.

The fluence for the 40 in. cores ranged from 1.40×10^{23} to 1.48×10^{23} nvt, and for the 36 in. cores from 1.47×10^{23} to 1.65×10^{23} nvt.

4.4 POWER SWING

The larger the change in the assembly power over a cycle, the greater the penalty in thermal performance of the reactor. While it is impossible to design a reactor that will run at a constant assembly power, it is always desirable to keep the change in assembly power as low as possible. Tables VII and VIII show how the peak rating in each core region changed over an equilibrium cycle. (These peak ratings were based on uncontrolled r-z calculations. The peak ratings from HEX calculations with control rod insertion for some of the most promising cores will be presented later.)

The outermost core region for the 40 in. and 36 in. cores always had the largest negative power swing. For the 40 in. cores, the power swing in this region could be as high as -23% or as low as -12.3%. The lowest swing was for the configurations with the largest number of isolated internal blanket assemblies in that region, i.e. configurations 12a, b and c. For 36 in. cores, the power swing in the outermost core region varied from -12.3% to -17.7%, with the reference core having the lowest swing.

While the power swings in the two inner core zones were also negative for all 36 in. cores analyzed they were in most cases positive for the 40 in. cores. The power swing in the first core region was more sensitive to changes in configuration than that in the second core region. The power swing in the first region ranged from -4.3% to +13.6% for the 40 in. cores and from -0.9% to -8.3% for the 36 in. cores.

The overall reactor power swing was generally more uniform for 36 in. cores than for 40 in. cores because the configurations for the former were more tightly coupled. Among the 36 in. cores, the reference core had the most uniform and, therefore, the lowest power swing. Of all the 40 in. cores, the lowest overall power swing was observed for configurations 12a, b, and c. The power swing for these cores was actually lower than most 36 in. cores.

4.5 POWER SHAPE SENSITIVITY

As a measure of the power instability caused by batch fuel enrichment uncertainties, Tables VII and VIII list the power sensitivity factor for the 40 in. and 36 in. cores. The power sensitivity factor is here defined as the percentage change in the peak assembly power in the innermost core region under BOL conditions due to a 0.5% change in the enrichment split for that core region. This power sensitivity factor is most useful in comparing the power instabilities of cores with about the same innermost core region size because

it depends on the number of fuel assemblies whose enrichment is perturbed. For cores with an identical innermost core region size, the higher the power sensitivity factor, the more unstable the power profile of the reactor.

Configurations 1 to 5 and the reference configuration for the 40 in. cores had 48 fuel assemblies in the first core region. The power sensitivity factor depended on the coupling between the second and third core regions as well as between the first and second core regions. It ranged from 2.41 to 2.91 for these configurations. Configuration 5 had the thinnest internal blanket rings and thus had the lowest power sensitivity factor.

The remaining configurations for the 40 in. cores had 36 fuel assemblies in the first core region, and the lowest power sensitivity factor (1.83) was obtained by configuration 11. Among the configurations that had a sodium void reactivity below $2.50, configurations 12a, b, and c had the lowest power sensitivity factor (1.85).

The power sensitivity factor for the 36 in. cores varies from 1.49 to 2.74. For those configurations with 48 fuel assemblies in the first core region, the only one with closed internal blanket rings, i.e. configuration 1, showed the highest sensitivity in power shape to enrichment changes. (This configuration had also a smaller center blanket region than the others.) The two remaining configurations (configuration 2 and the reference configuration) had 60 or 72 fuel assemblies in the first core region and they both had a closed-ring arrangement. Their power sensitivity factors were significantly higher than those of the configurations with a smaller first core region. The lowest power sensitivity factor for the 36 in. cores with sodium void reactivities below $2.50, was 1.95 for configuration 5.

4.6 BREEDING

In the breeding performance analysis, the fuel and internal blanket residence time was fixed to two years. The radial blanket assemblies stayed in the reactor for 5 years. The reactor was refueled annually with a 70% load factor. Tables IX and X list the breeding performance of all the 40 in. and 36 in. cores analyzed. The breeding ratio for both core heights showed little variation from configuration to configuration. While the breeding ratio was generally somewhat higher for the 40 in. cores, the reactor doubling time and compound system doubling time were usually shorter for the 36 in. cores because the latter have lower fissile inventories. The shortest compound system doubling time for the 40 in. cores was 15.6 years for configuration 11. For

the 36 in. cores, configuration 3 had the shortest compound system doubling time of 15.1 years. The longest compound system doubling time for the 40 in. and 36 in. cores was 16.4 and 15.7 years, respectively. Using the assembly size and configuration of configuration 5 but increasing the core height to 42 in. (see Section 4.1) increased the compound system doubling time by 0.5 years.

Reactor doubling times were approximately 2 years shorter than compound system doubling times.

4.7 SODIUM VOID REACTIVITY

The sodium void reactivities listed in Tables IX and X for voiding the flowing sodium in the core and upper axial blanket regions were based on first order perturbation calculations. With the exception of configurations 4 and 11, all the 40 in. cores had a sodium void reactivity below $2.50. The reference configuration had the lowest sodium void reactivity of $2.19. For the 36 in. cores, the reference configuration and configurations 4 and 5 had sodium void reactivities between $2.23 and $2.29. The other configurations lead to sodium void reactivities exceeding $2.50. Increasing the core height from 36 in. to 42 in. but keeping the core layout and assembly size the same as that of configuration 5, resulted in a $0.34 increase in sodium void reactivity.

In general, for a given core height, the smaller the sodium void reactivity, the longer the doubling time. But differences from this trend were seen in the 40 in. cores with 12a, b, and c configurations. These cores had, with the exception of configuration 11, the shortest doubling time, yet their sodium void reactivities ($2.38) were lower than most of the other 40 in. cores.

5.0 SELECTION OF MOST PROMISING CONFIGURATIONS

The selection of optimized core configurations was constrained by the $2.50 sodium void reactivity limit. Only those cores that were able to meet this limit were given further consideration. Among those configurations, the major criteria for the optimization were (1) the sensitivity of the power shape to slight changes in enrichment split and (2) the maximum power swing in a fuel assembly over a burnup cycle. The criteria for the optimization of configurations were then in their order of importance,

- doubling time
- specific inventory
- burnup swing

The burnup swing determined to a great extent the control system requirements and the maximum reactivity fault that could result from an accidental control rod withdrawal and thus was taken into consideration in the optimization.

While the maximum allowable sodium void reactivity was set to be $2.50, one should keep in mind that the sodium void reactivity direct eigenvalue calculations as opposed to perturbation calculations was $\sim$ 10¢ greater for sodium void reactivities in the $2.00 to $2.50 range. The cut-off limit for the sodium void reactivity for the cores listed in Tables IX and X was, therefore, approximately $2.40.

5.1 40 IN. HIGH CORES

Because of the $2.40 limit on the sodium void reactivity, configurations 2, 4, 5, 6, 7, 8, and 11, were disqualified. Among the remaining configurations, configurations 12a, b, and c which were identical with respect to performance characteristics based on r-z calculations, exhibited the least sensitivity in power shape to small enrichment split changes as well as the lowest power swing (Table VII). In addition they had the lowest doubling time (15.7 years), even though the variations were $\leq$ 0.7 years. Only configuration 9 had a slightly lower specific inventory than these configurations, (Table III). The burnup swing of 0.49% for these configurations was the lowest for 40 in. cores, including those that did not meet the sodium void reactivity requirement. The choice of the optimum configuration for 40 in. cores was obviously from among 12a, b, and c.

Configurations 12a, b, and c were quite similar. Except for the rearrangement of the 12 control rods within the first two core regions, configuration 12b was identical to 12a. The fourth internal blanket region of isolated blanket assemblies in configuration 12c was arranged slightly different from 12b. Otherwise, configurations 12b and c were identical. For the performance analysis of these three configurations using the hexagonal geometry models, the row 11 control rods were inserted. These control rods were selected for reactivity control for two reasons. First, the outermost core region had the highest power swing. By inserting control rods located in this region and then withdrawing them during the cycle to compensate for the reactivity loss reduces the power swing in this region. Secondly, the row 11 control rods were located at the peak power positions. The local power peaking in the outermost core region was minimized when these control rods were inserted.

The assembly-wise peak power density for configurations 12a, b, and c is shown in Figs. 22 to 24 for BOEC conditions, and in Figs. 25 to 27 for EOEC conditions. The region-wise peak and peak-to-average ratings at various burnup stages are listed in Table XII. The peak-to-average rating in the largest, outermost core region was lowest for configuration 12c at any stage. The peak-to-average ratings in the other core regions for this configuration were close to, though not, the lowest. As a consequence, for a given reactor power configuration 12c had a lower peak reactor rating than either 12a or b. (The BOL peak reactor ratings were 13.88, 13.70 and 13.39 kW/ft, respectively, for configurations 12a, b, and c.)

The uncontrolled power swing over the equilibrium cycle in the outermost core region was -12.3% for the three configurations (Tables VII). It was reduced to approximately -2% when the row 11 control rods were inserted for criticality control.

The control rod worths shown in Table XIII for configuration 12a, b, and c were based on the CRBR control rod composition with 90% enriched boron. The primary control system in all the cases included, in addition to the 6 row 11 rods, the 6 row 7 rods. The remaining 12 served as the secondary control rods. (The worth of the primary system was calculated with all the primary rod inserted simultaneously. The worth of the secondary system was calculated in a similar fashion but with the row 11 primary rods initially partially inserted to account for interactions between the primary and secondary rods.) The combined worth of both systems differed only

slightly for the three configurations. However, the primary control system for configuration 12c had the greatest margin in worth over the secondary system. From the viewpoint of control rod allocation configuration 12c is again most desirable.

With the best power peaking characteristic and the ease with which control rods can be allocated configuration 12c was chosen over 12a and 12b as the optimum core layout for the 40 in. system.

5.2 36 IN. HIGH CORES

For the 36 in. cores shown in Table X, configurations 4 and 5 and the reference configuration had sodium void reactivities within the $2.40 cut-off limit. While the reference configuration had closed internal blanket rings, configurations 4 and 5 employed broken-ring arrangements. None of the three configurations showed clear advantages or disadvantages with respect to the power shape sensitivity, power swing and breeding. However, configuration 4 was eliminated as a possible choice as the optimum configuration for 36 in. cores because it revealed such a high power peaking in the outermost core region near the blanket opening that no control rod insertion pattern could effectively reduce the abnormal power distribution. This exceedingly high power peaking was the reason configuration 5, which had a modified outermost core region and modified control rod locations, was developed in the first place.

While Table VIII shows a higher power sensitivity factor for the reference configuration than for configuration 5, one should keep in mind the power sensitivity factor as it was defined depended not only on the coupling but also on the number of fuel assemblies to which the enrichment perturbation was applied. A comparison of power shape sensitivity should not be rigorously pursuited based solely on the power sensitivity factor for core designs that had vastly different core region sizes.

Between the reference configuration and configuration 5 for the 36 in. cores, differences in the power swing, doubling time, specific inventory and burnup swing were so small that the selection of the final core layout could not be based on these criteria. Instead, the decision had to come from the fundamental characteristics in power peaking and control simplicity associated with the closed- and broken-ring arrangements.

The BOL assembly-wise peak power densities for the two configurations are shown in Figs. 28-31. Without control rod insertion, the reference configuration showed a more uniform power distribution than configuration 5. However,

in actual operation certain control rods have to be inserted to offset the reactor excess reactivity. The power distribution shown in Figs. 30 and 31 are for the case when the corner control rods in the outer core region of the two cores were fully inserted. The power distribution then became more uniform for configuration 5. The outer core corner control rods (in row 12 for the reference configuration and in row 11 for configuration 5) were selected for burnup control because they were near the peak power assemblies and they could be used to compensate for the high power swing occurred in the outer core region.

For configuration 5, these control rods were sufficient to maintain reactor criticality. For the reference configuration, on the other hand, a second control rod bank was required because the closed-ring arrangement reduced substantially the worth of these rods, even though they remained the highest worth rods. Control simplicity and the power peaking performance both favored configuration 5. It was, therefore, selected as the optimum core layout for the 36 in. system.

6.0 SUMMARY AND CONCLUSIONS

Two promising core configurations, one for a 40 in. core with 0.26 in. fuel pins, and one for a 36 in. core with 0.24 in. fuel pins were obtained through a series of core layout modifications. The analysis of various core layouts which differed with respect to coupling, core region size, internal blanket arrangement but retained the original center-blanket, three core region arrangement lead to the following conclusions:

(1) The design constraints of
   a. $\leq$ \$2.50 sodium void reactivity
   b. $\leq$ 15 year doubling time
   are very restrictive

(2) The selection of configuration is very important in regard to
   a. sodium void reactivity
   b. power shape sensitivity
   c. power swing
   d. burnup swing and control requirements

(3) The following performance parameters are also affected by the configuration selection but to a lesser extent
   a. specific inventory
   b. breeding ratio
   c. doubling time

(4) For a given core height, tightly coupled configurations generally perform better than loosely coupled configurations with respect the performance parameters listed in (2) except for the sodium void reactivity.

(5) The region size split among the three core regions is important for sodium void reactivity reductions.

(6) The highest power swing over a burnup cycle exists in the outermost core region. This region has always a negative power swing.

(7) The introduction of isolated internal blanket assemblies in the outermost core region
   a. lessens the need for loosely coupled systems to achieve a given sodium void reactivity
   b. reduces the power shape sensitivity
   c. leads to lower power and burnup swings

(8) Broken ring arrangements are better than closed ring arrangements because
   a. there is better coupling between regions
   b. flux peaks are created which
      - determine the location of control rods
      - enhance control rod worth

(9) Control rod positioning is very important
   a. burnup can be controlled very efficiently by control rods located in the outermost core region because
      - outermost core region is the largest core region which makes a symmetrical arrangement less difficult
      - the withdrawal of control rods counteracts the drop in assembly power observed in cores burned without control
   b. control rods located next to an internal blanket region have a lower worth than control rods surrounded by fuel assemblies except for the outermost core region where for some configurations the worth of the control rod can be higher when placed next to an internal blanket assembly.

(10) While there is the potential for arranging the internal blanket assemblies such that only one core enrichment is needed, no extensive efforts were undertaken at this stage to develop such a core because of
   a. calculational uncertainties
   b. having different enrichment zones is a more conservative approach

(11) The choice of calculational techniques is very important
   a. r-z models are good for
      - inventory calculation
      - breeding performance calculation
      - sodium void reactivity estimates

b. hexagonal geometry models are needed for the calculation of
   - all power shape information
   - control rod worth

The two most promising core configurations chosen are both tightly coupled, although one evolved from a loosely coupled core. Both cores showed low power shape sensitivities to smaller enrichment split changes and low power and burnup swings and good power peaking characteristics. They nearly reached the design goal of 15 years for doubling time. The performance characteristics of the two cores are compared in detail in the main report, where the selection of the final optimum core is made.

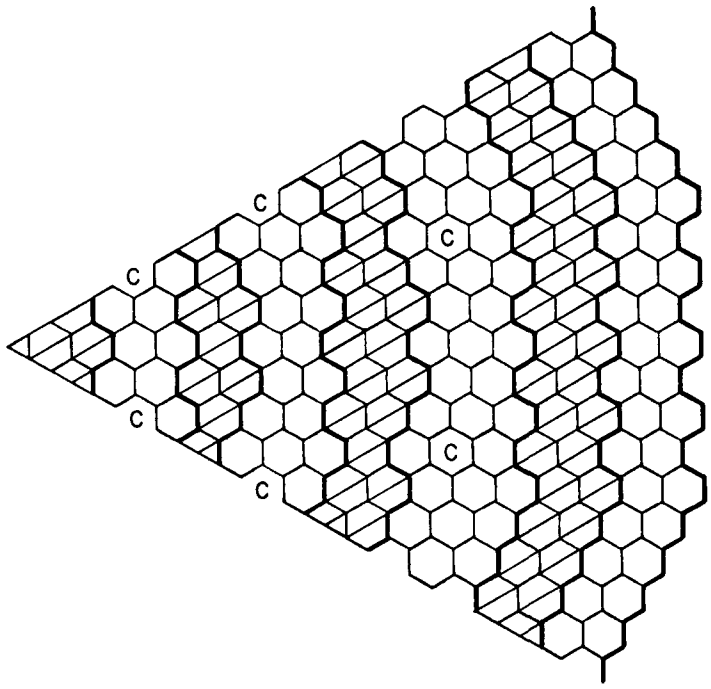

Fig. 1. Layout for 40 in. Core - Reference Configuration

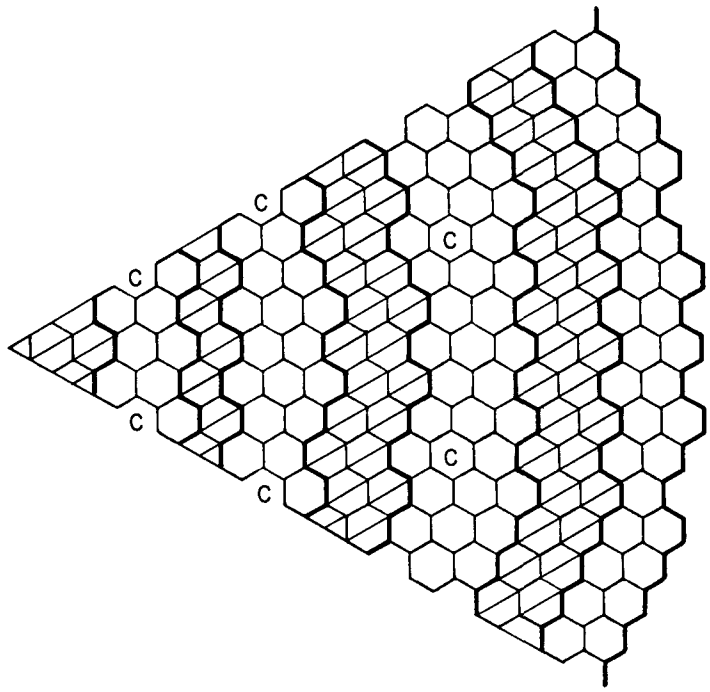

Fig. 2. Layout for 40 in. Core - Configuration 1

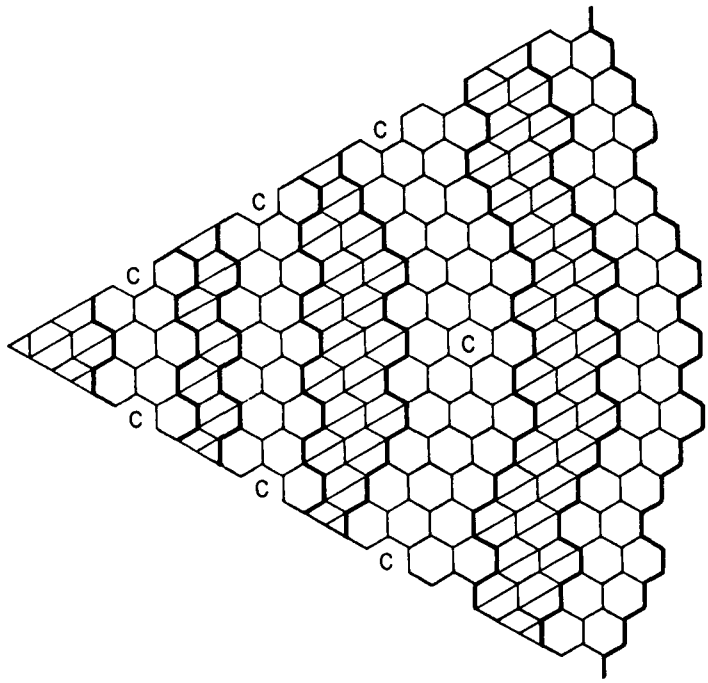

Fig. 3. Layout for 40 in. Core - Configuration 2

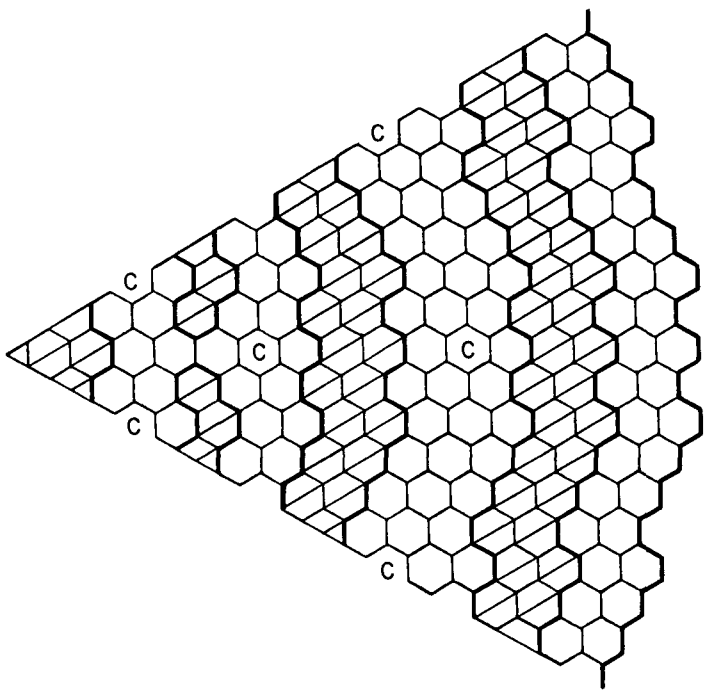

Fig. 4. Layout for 40 in. Core - Configuration 3

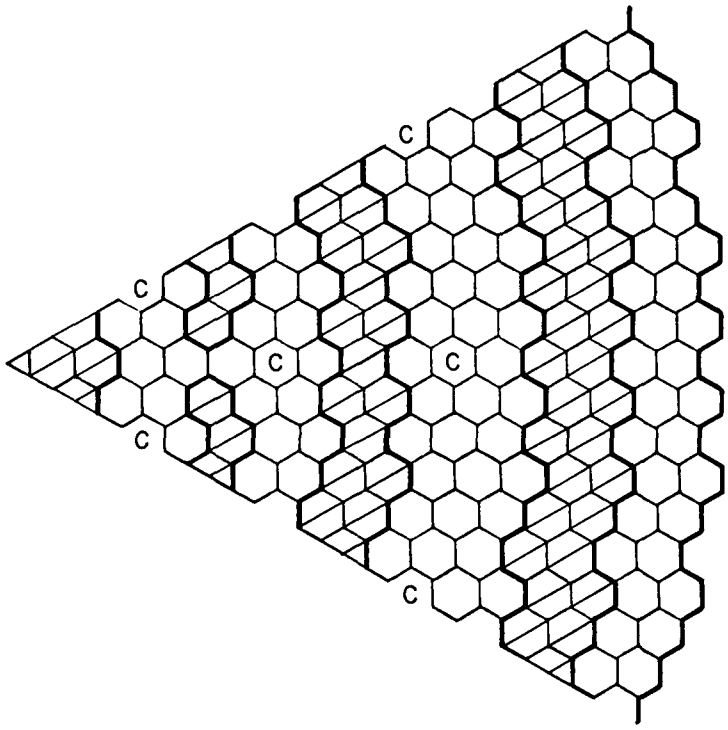

Fig. 5. Layout for 40 in. Core - Configuration 4

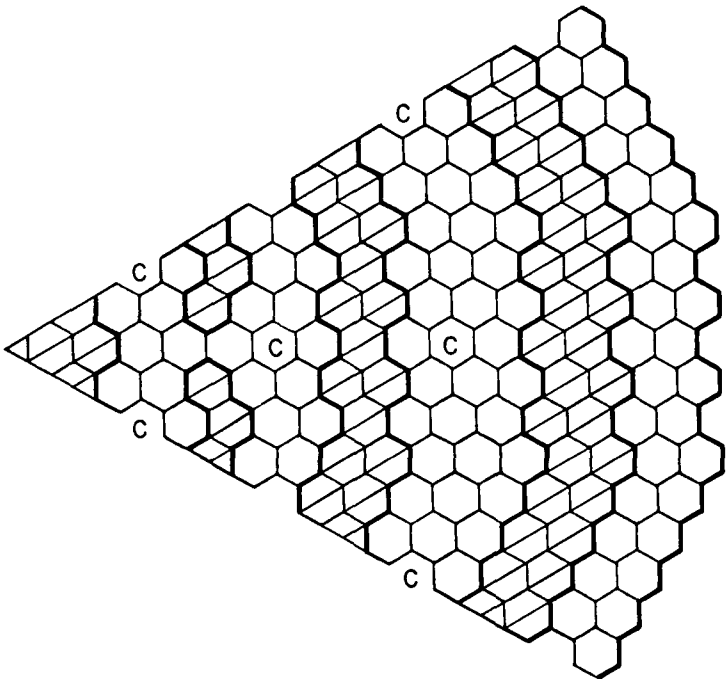

Fig. 6. Layout for 40 in. Core - Configuration 5

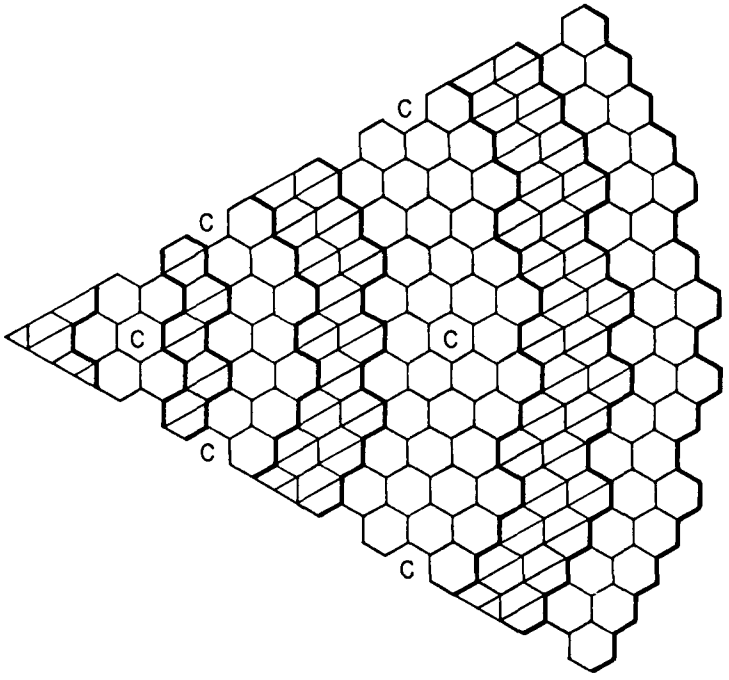

Fig. 7. Layout for 40 in. Core - Configuration 6

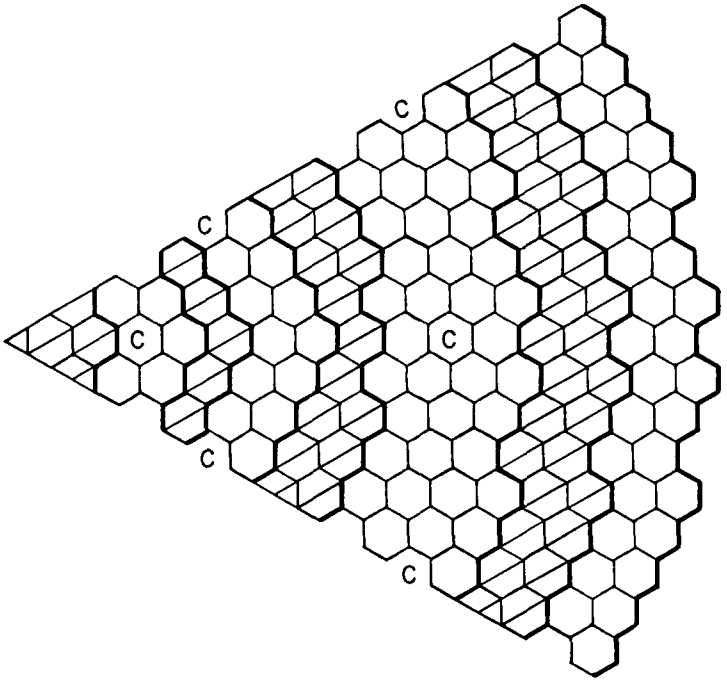

Fig. 8. Layout for 40 in. Core - Configuration 7

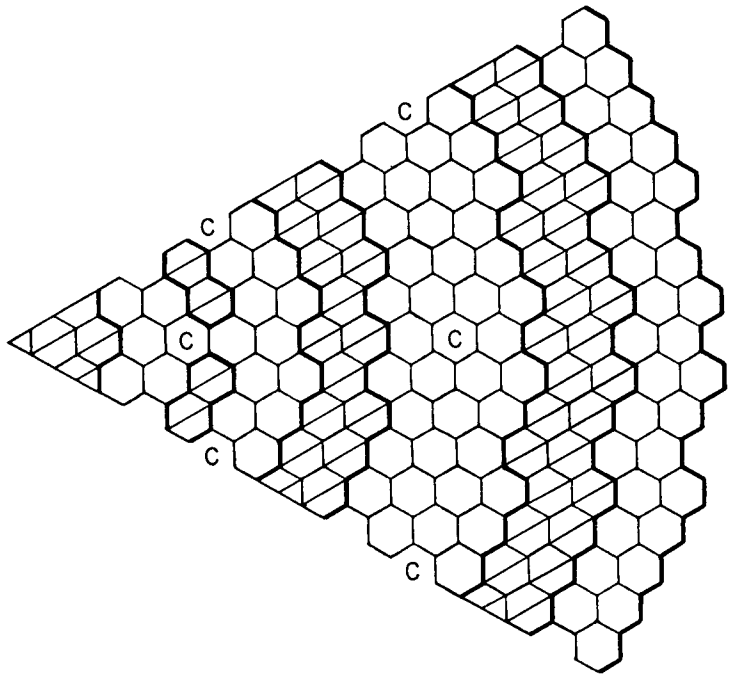

Fig. 9. Layout for 40 in. Core - Configuration 8

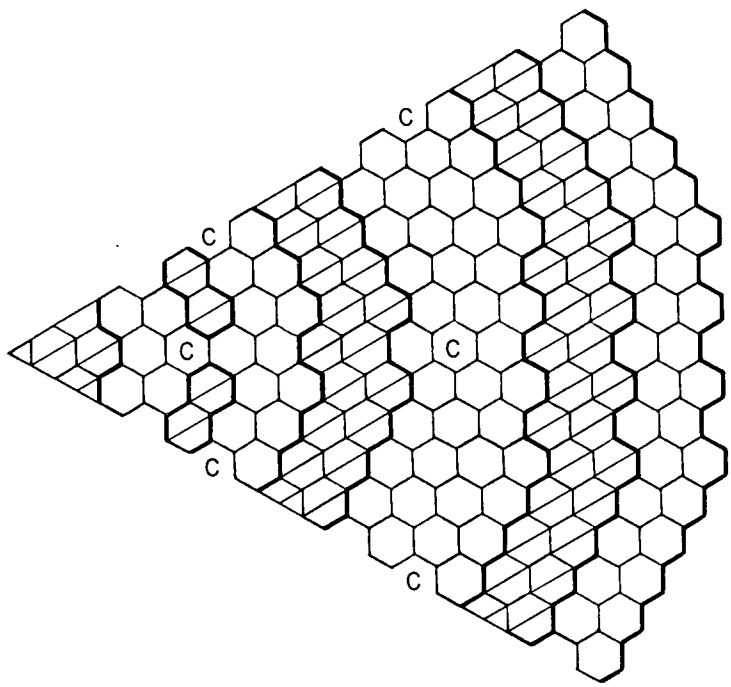

Fig. 10. Layout for 40 in. Core - Configuration 9

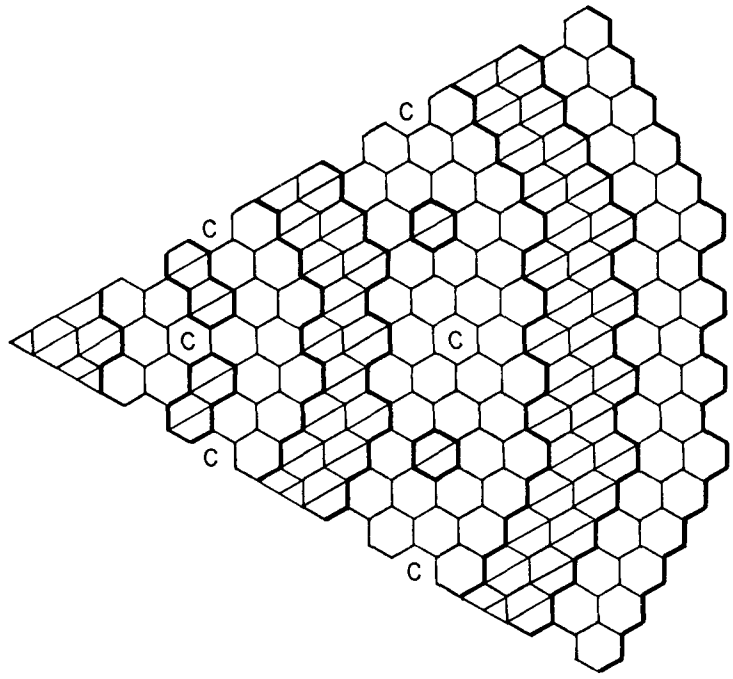

Fig. 11. Layout for 40 in. Core - Configuration 10

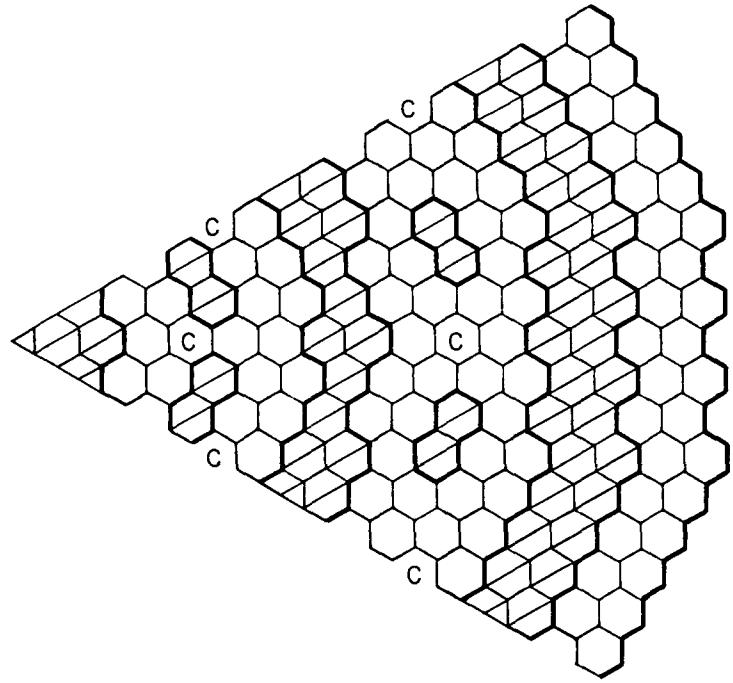

Fig. 12. Layout for 40 in. Core - Configuration 11

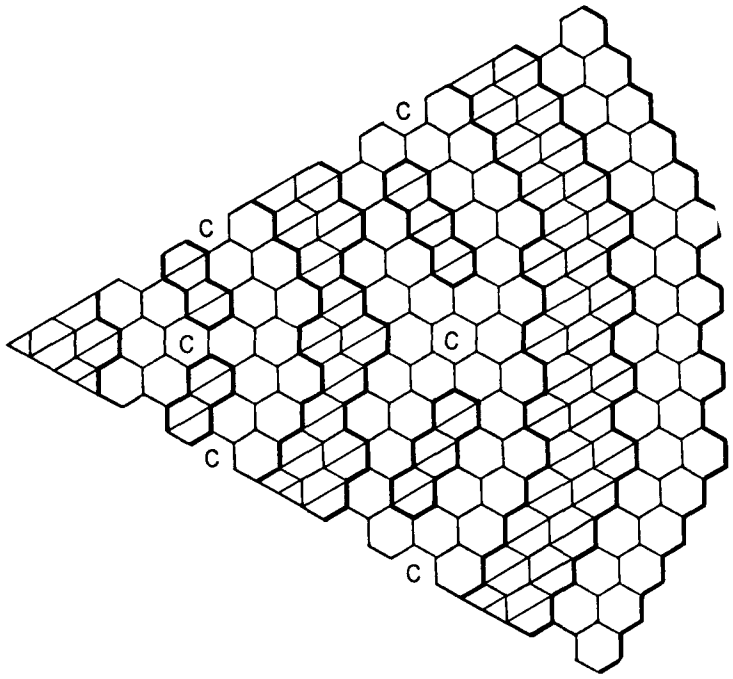

Fig. 13. Layout for 40 in. Core - Configuration 12a

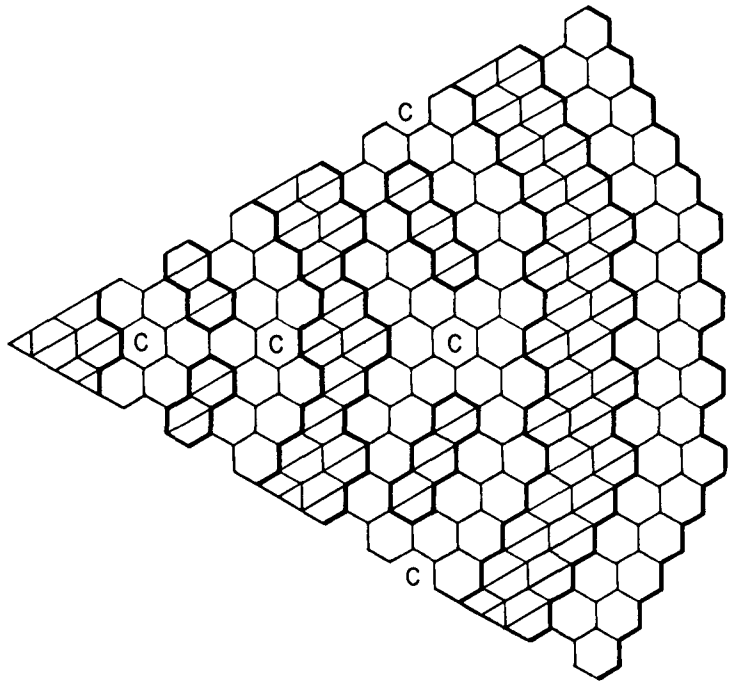

Fig. 14. Layout for 40 in. Core - Configuration 12b

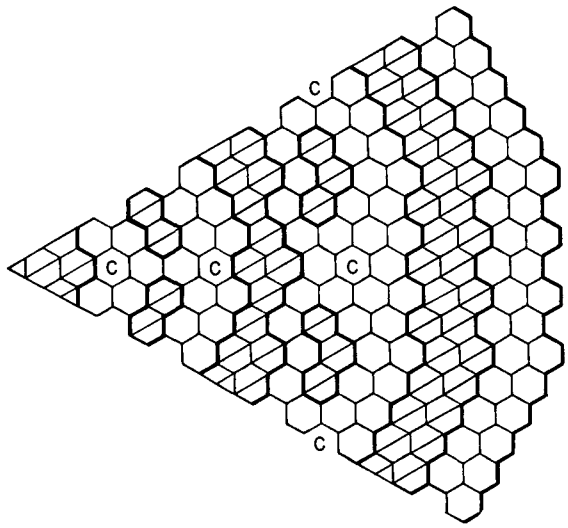

Fig. 15. Layout for 40 in. Core - Configuration 12c

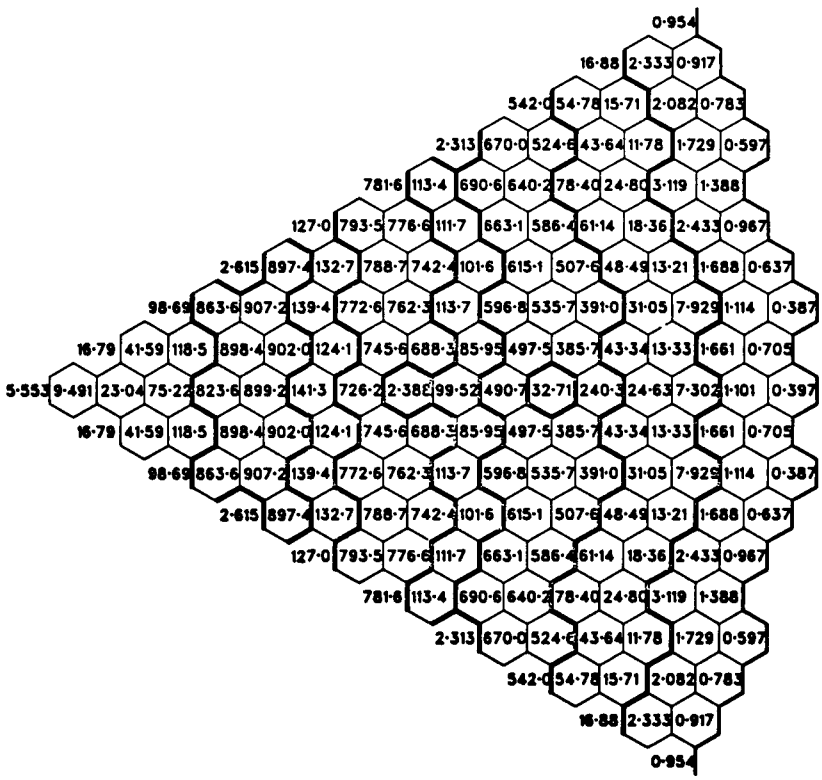

Fig. 16. Layout for 36 in. Core - Reference Configuration

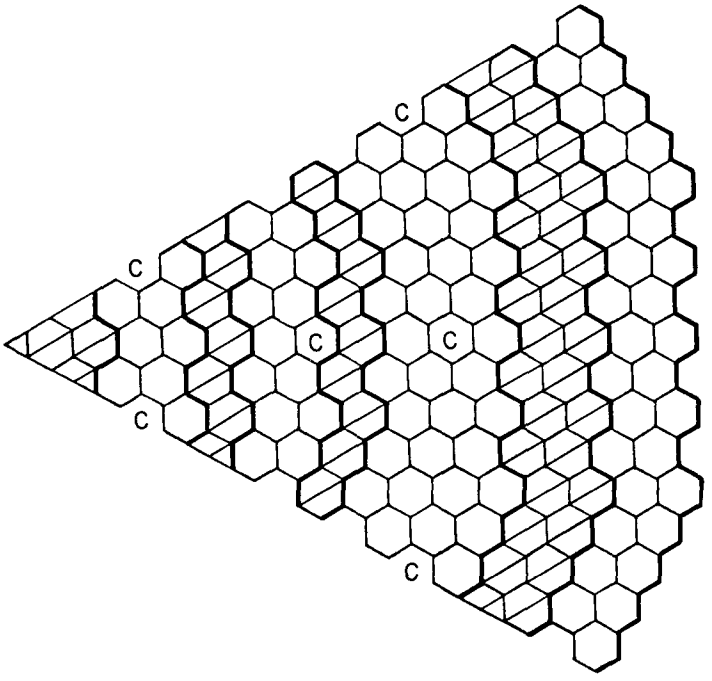

Fig. 17. Layout for 36 in. Core - Configuration 1

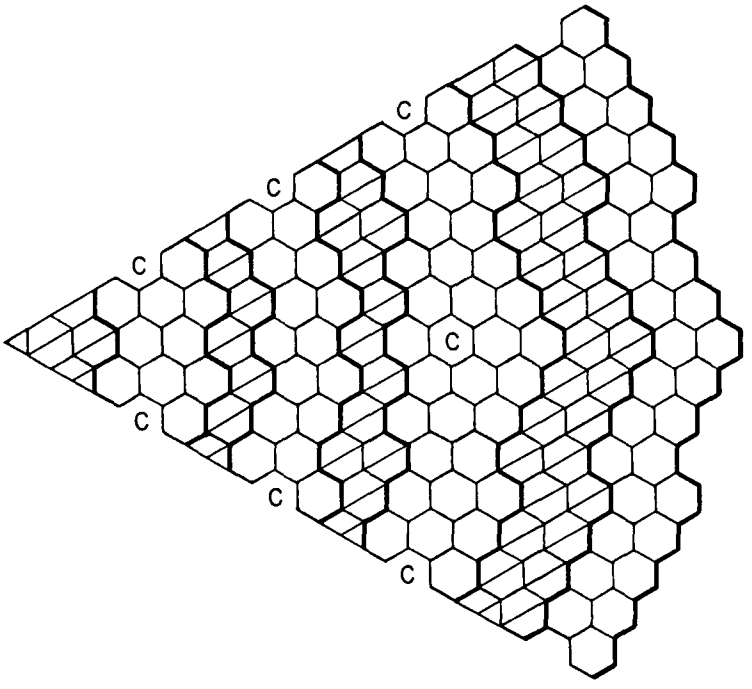

Fig. 18. Layout for 36 in. Core - Configuration 2

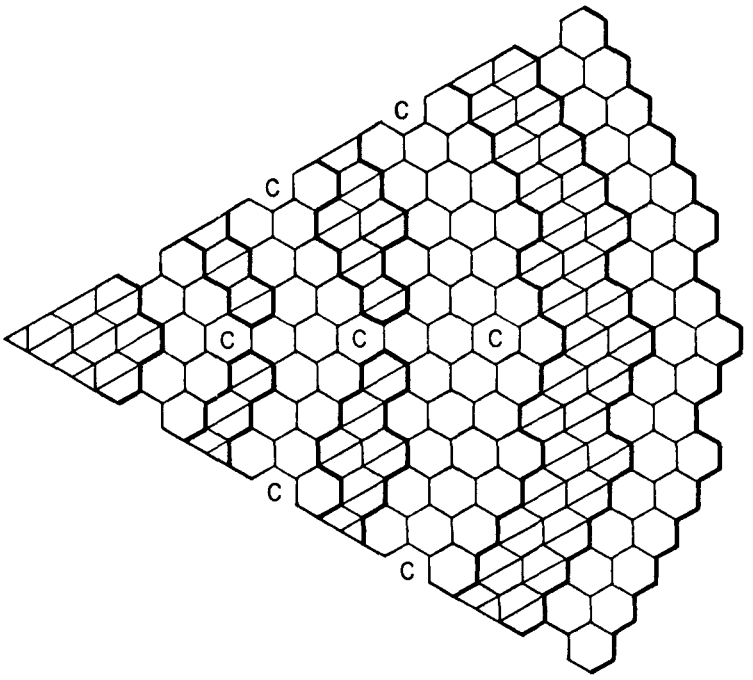

Fig. 19. Layout for 36 in. Core - Configuration 3

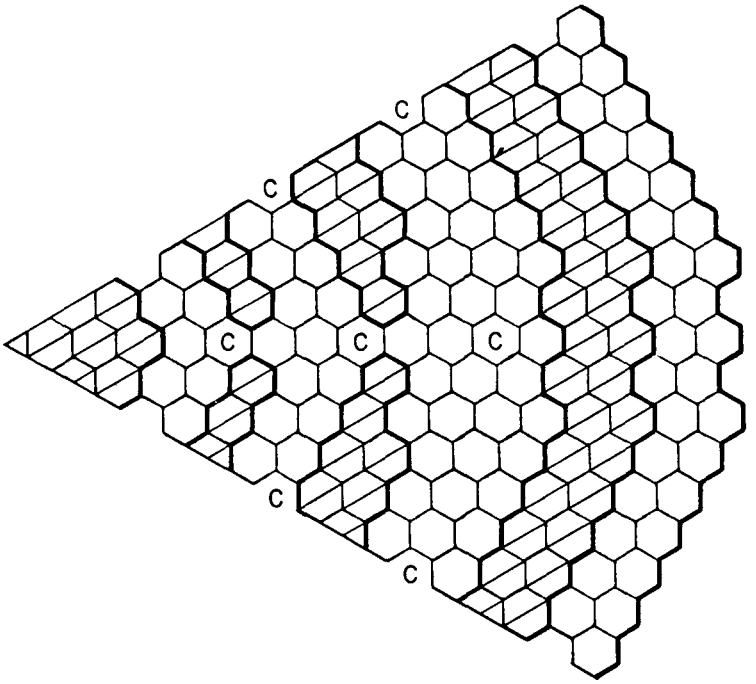

Fig. 20. Layout for 36 in. Core - Configuration 4

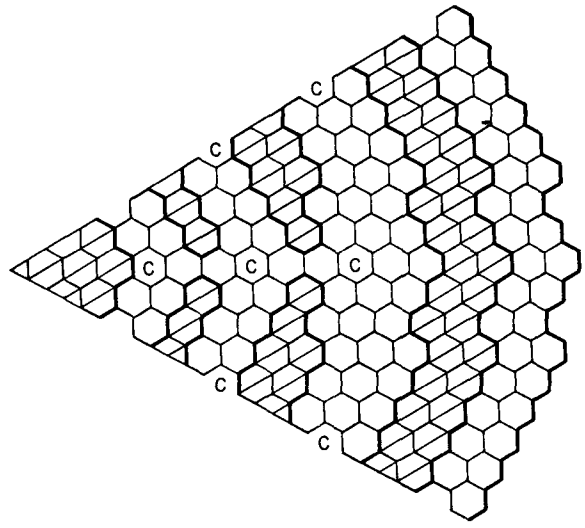

Fig. 21. Layout for 36 in. Core - Configuration 5

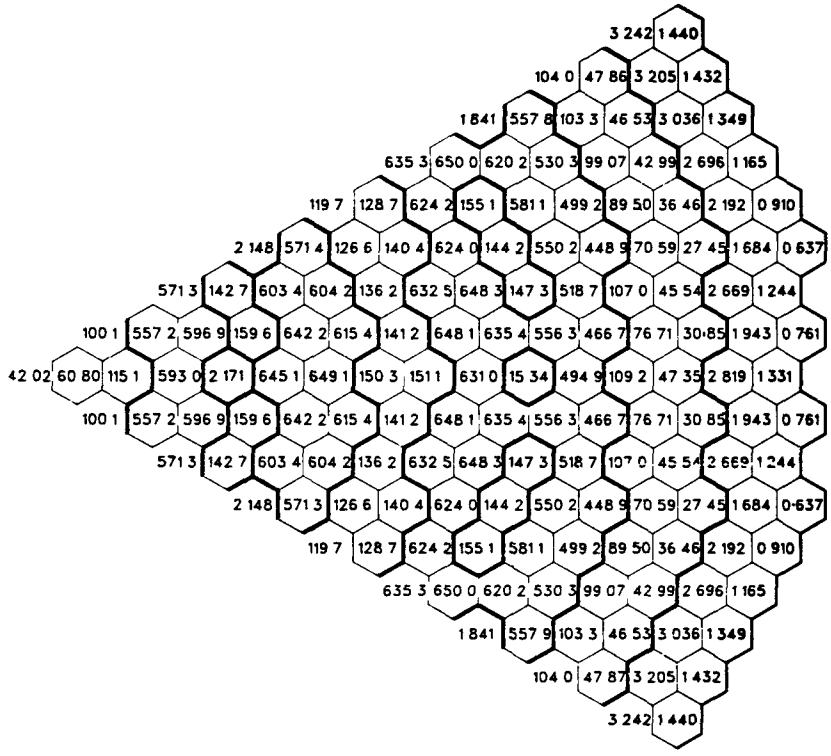

Fig. 22. BOEC Assembly-Wise Peak Power Density for Configuration 12a 40 in. Core

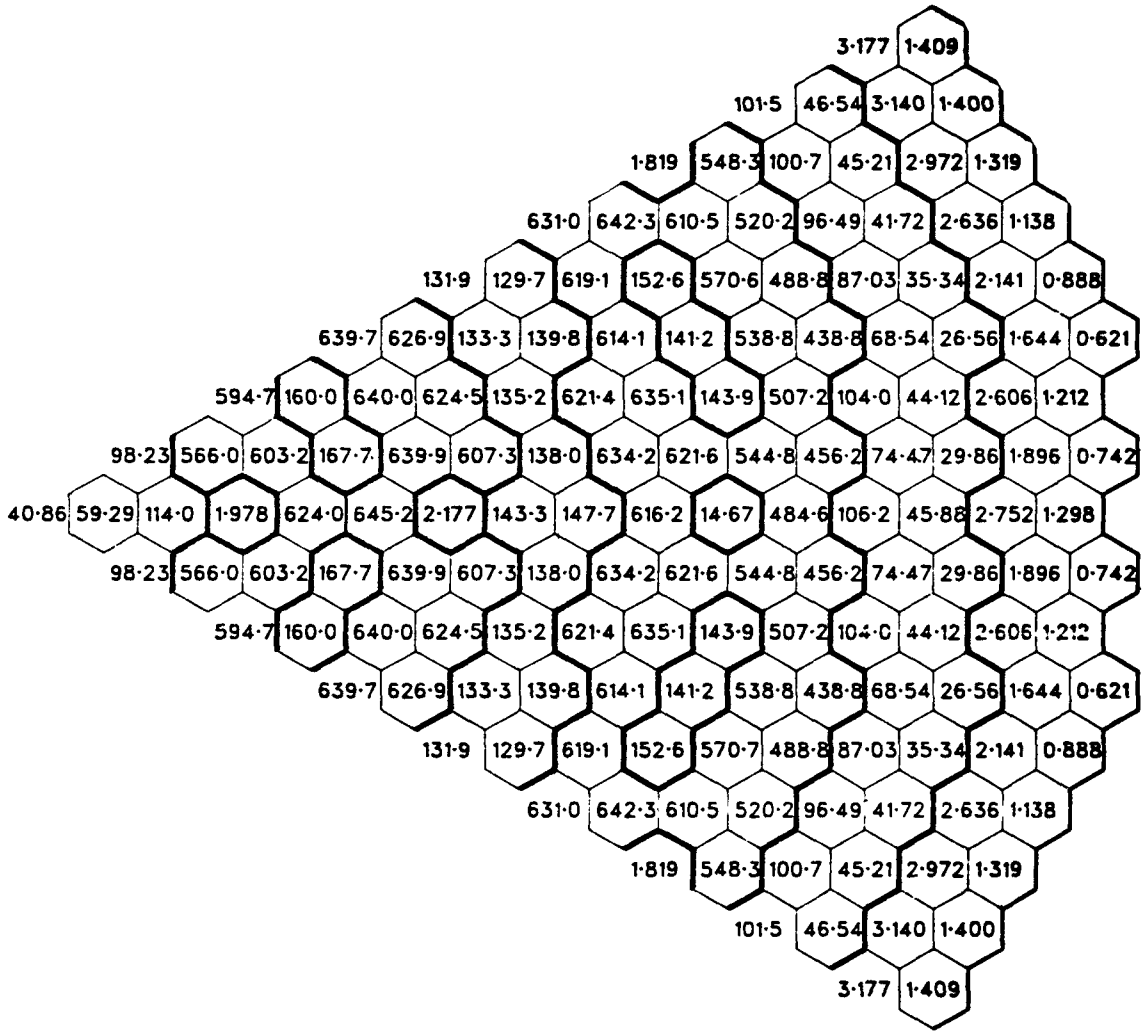

Fig. 23. BOEC Assembly-Wise Peak Power Density for Configuration 12b 40 in. Core

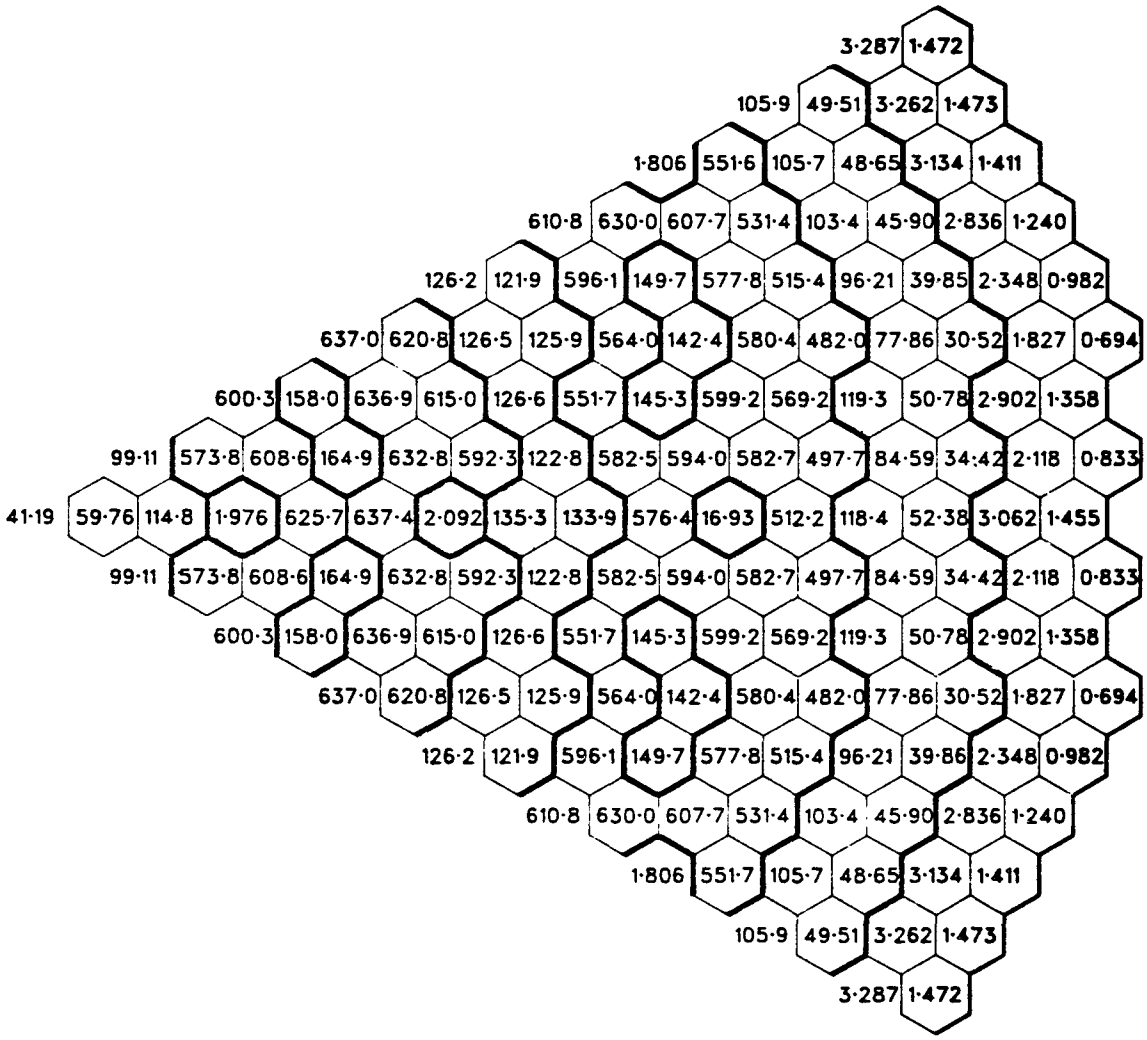

Fig. 24. BOEC Assembly-Wise Peak Power Density for Configuration 12c 40 in. Core

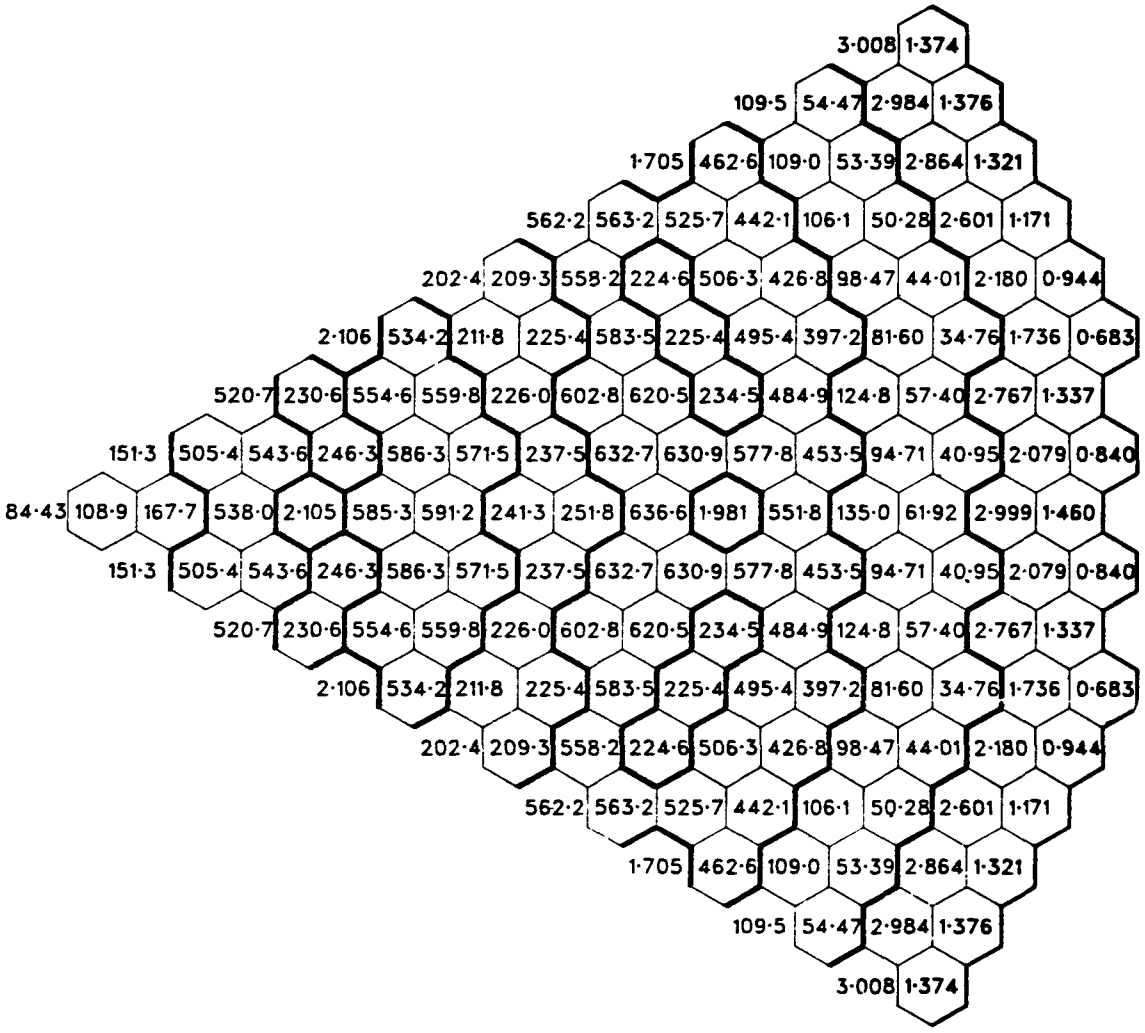

Fig. 25. EOEC Assembly-Wise Peak Power Density for Configuration 12a 40 in. Core

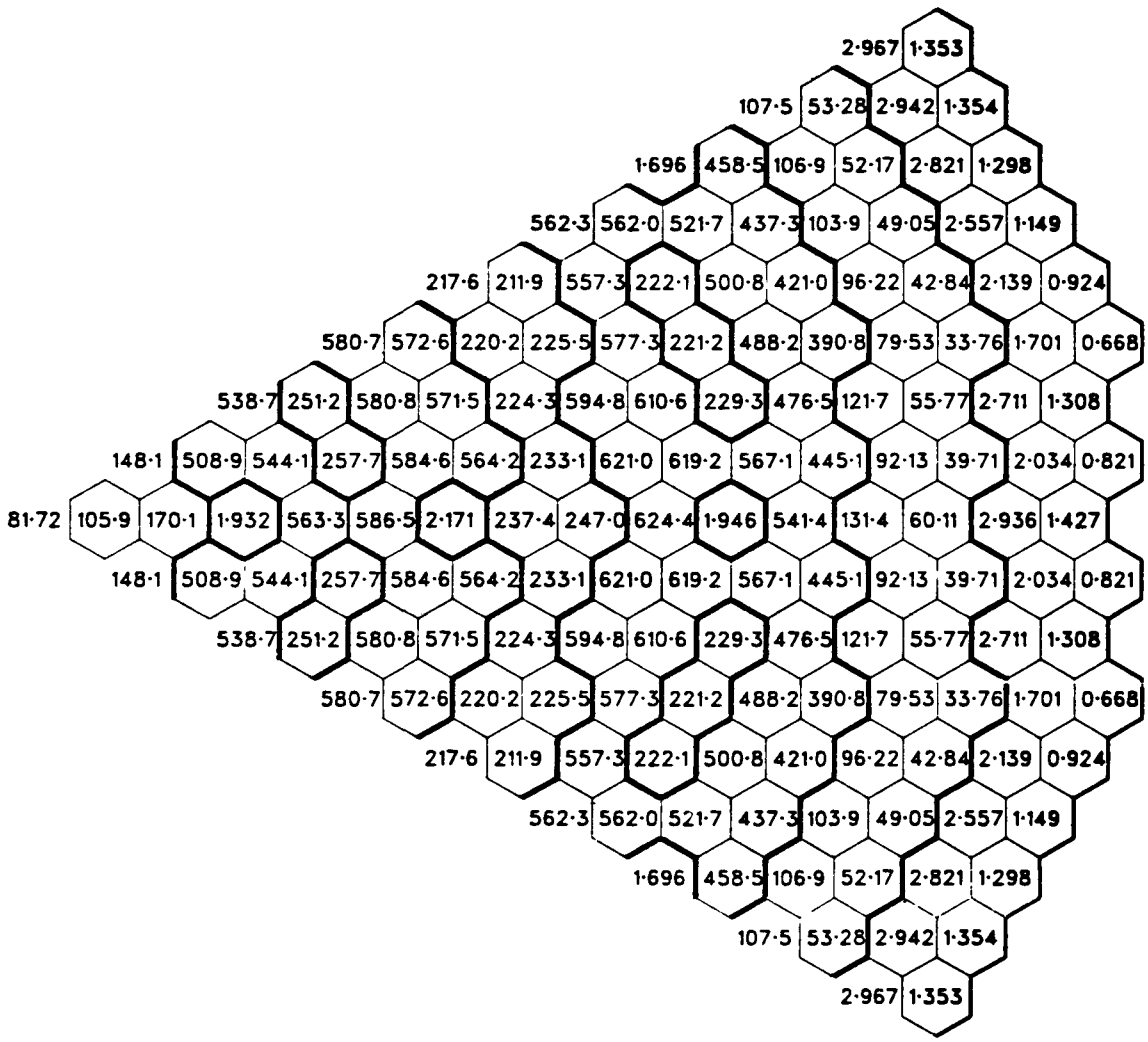

Fig. 26. EOEC Assembly-Wise Peak Power Density for Configuration 12b 40 in. Core

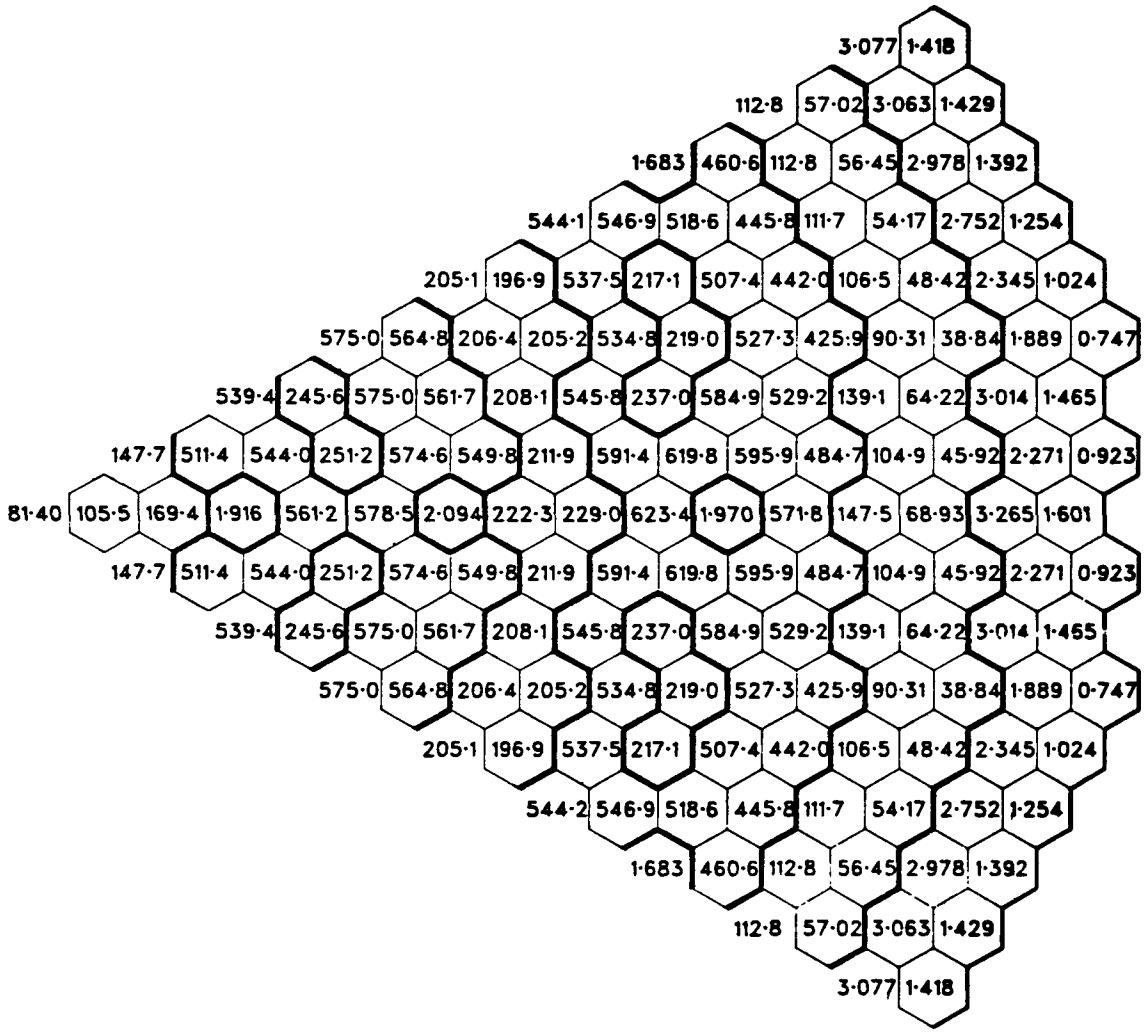

Fig. 27. EOEC Assembly-Wise Peak Power Density for Configuration 12c 40 in. Core

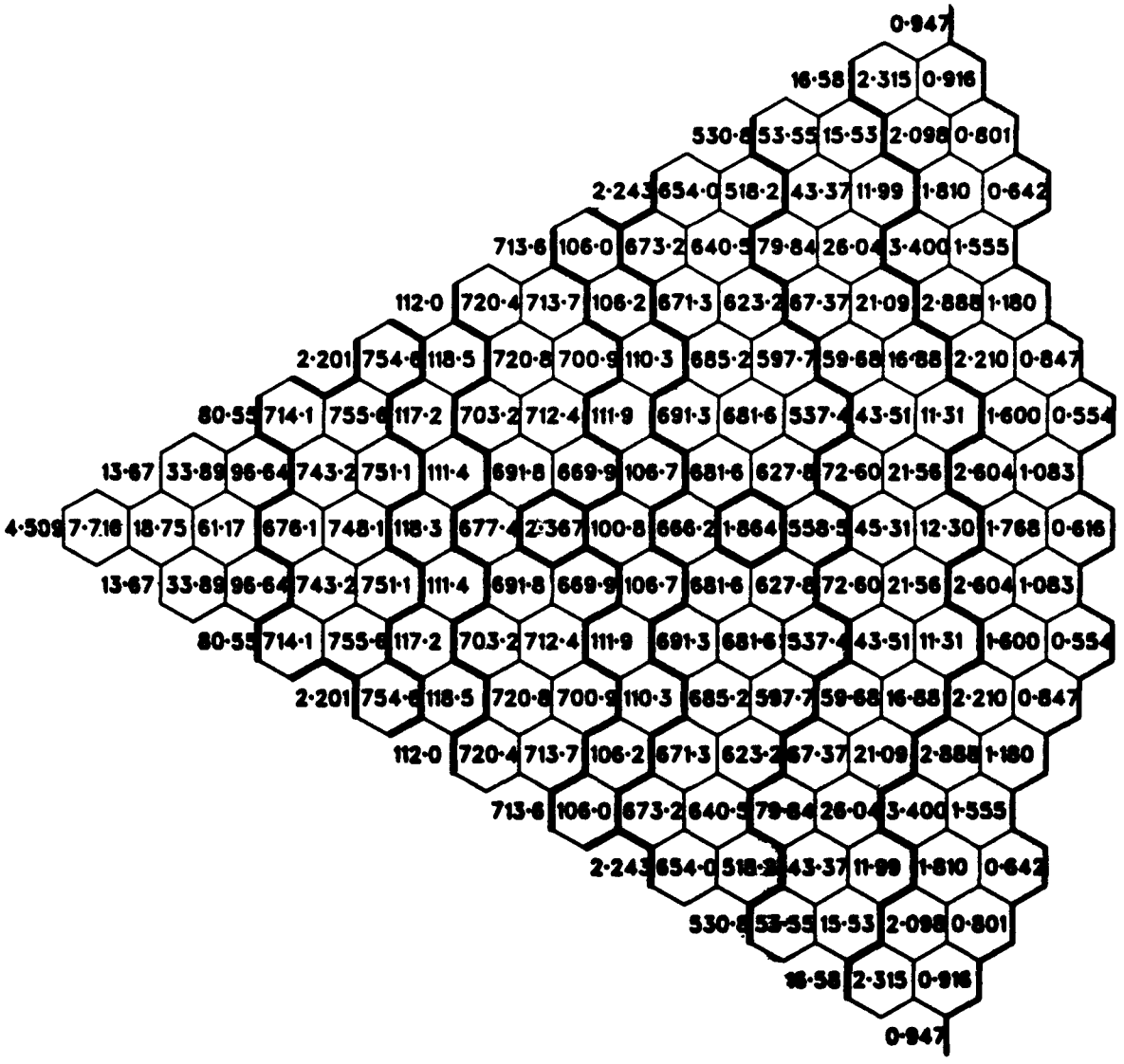

Fig. 28. BOL Assembly-Wise Peak Power Density for Reference 36 in. Core - All Rods Out

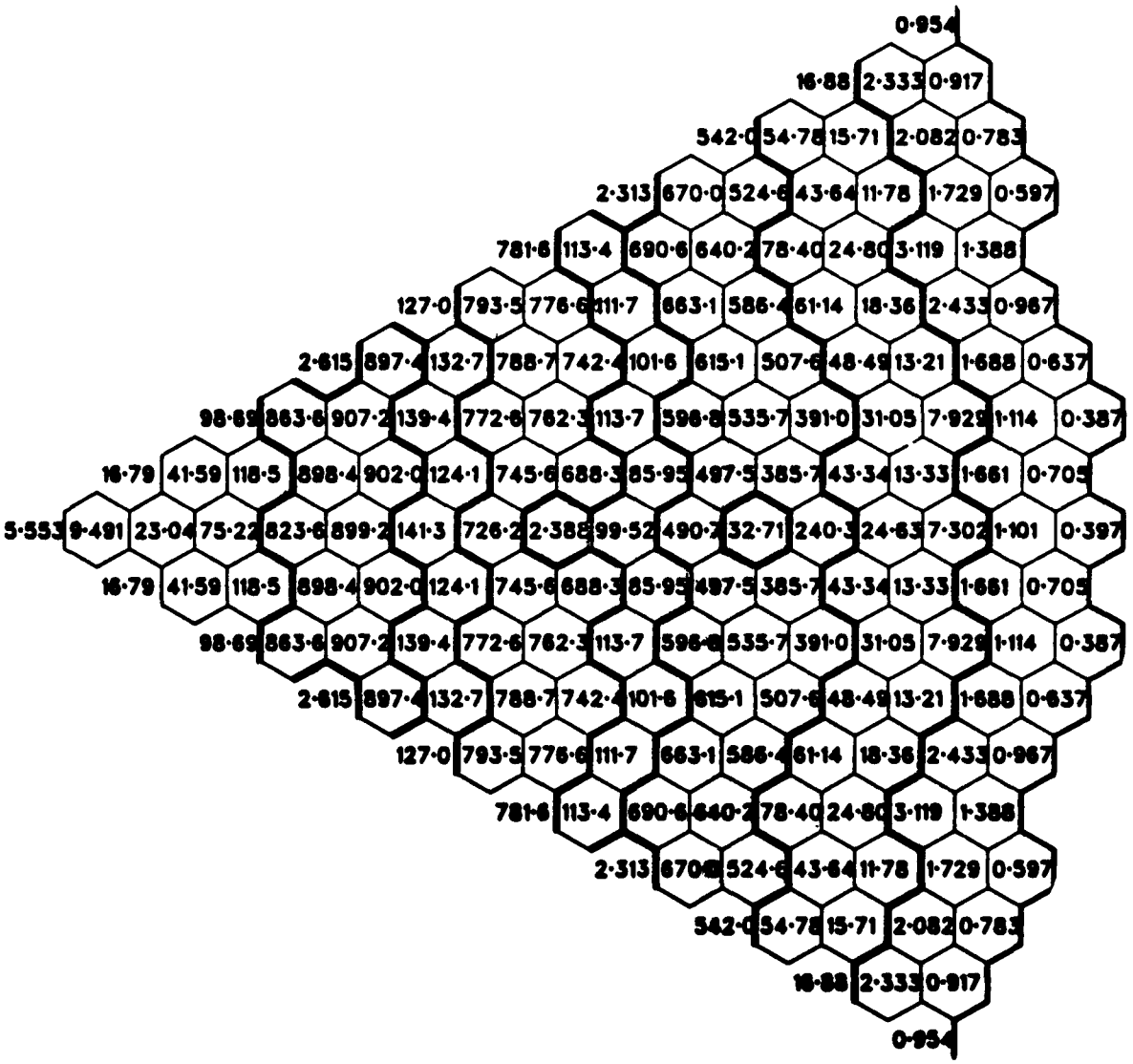

Fig. 29. BOL Assembly-Wise Peak Power Density for Reference 36 in. Core - Row 11 Rods In

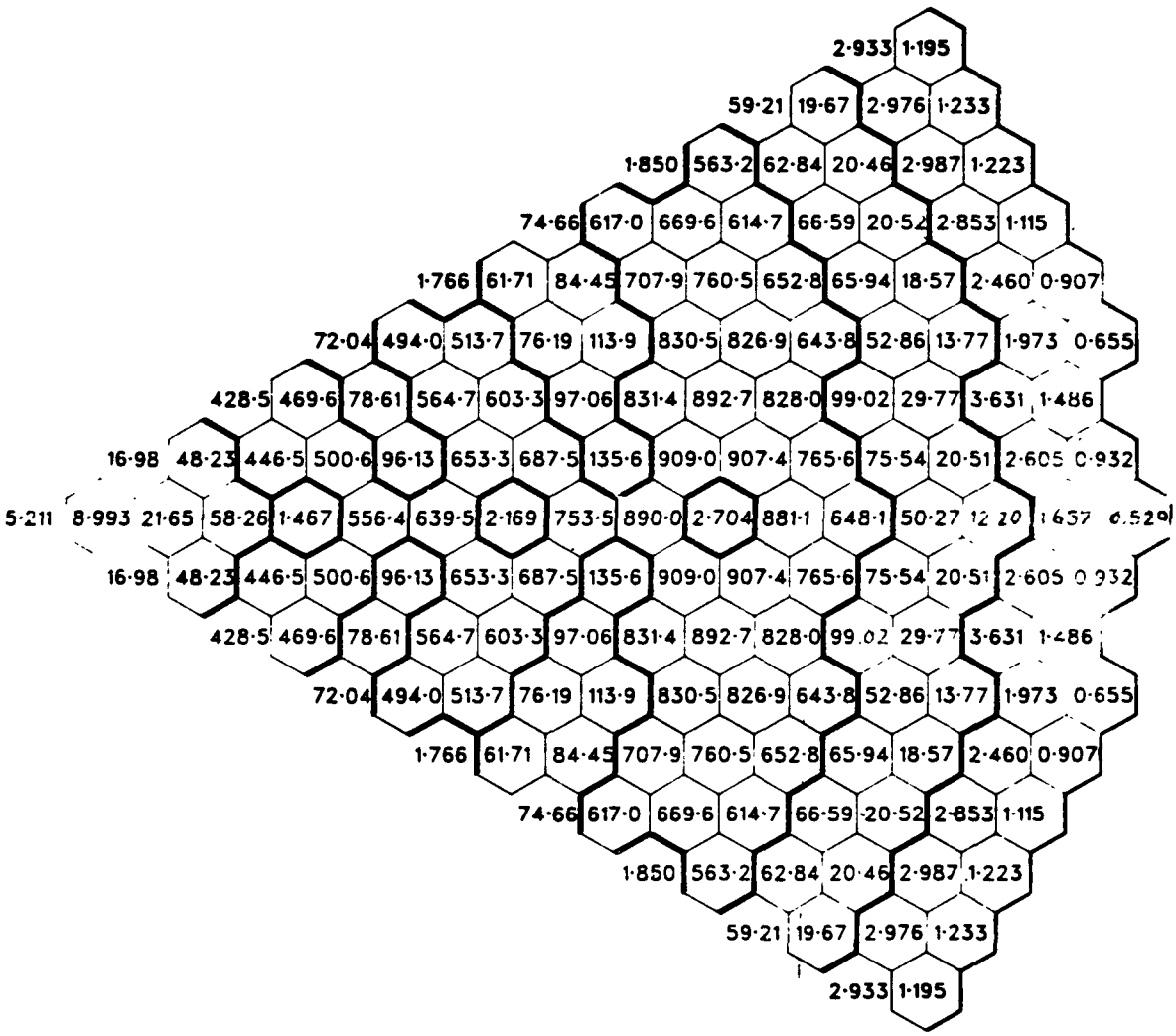

Fig. 30. BOL Assembly-Wise Peak Power Density for Configuration 5 36 in. Core - All Rods Out

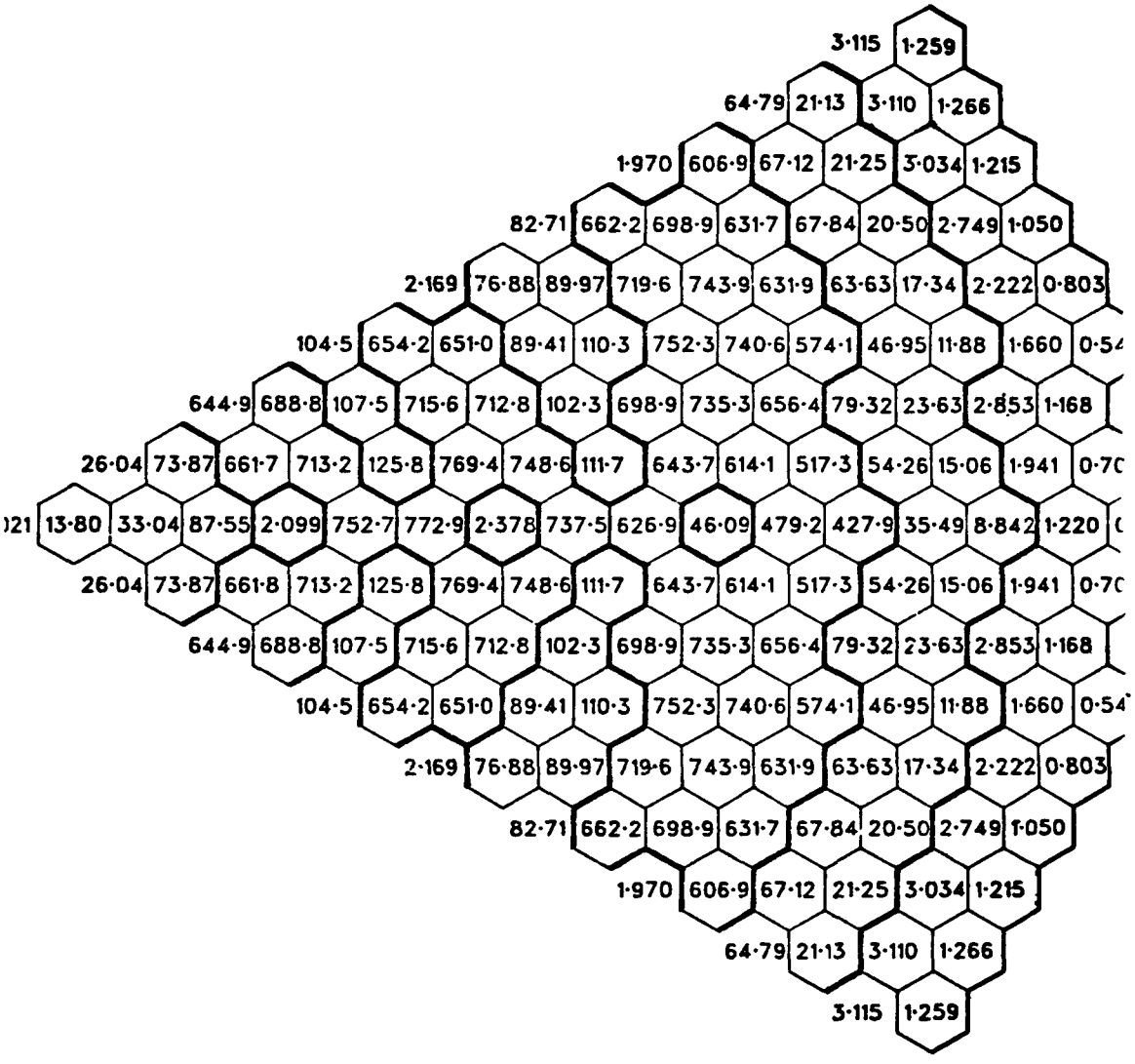

Fig. 31. BOL Assembly-Wise Peak Power Density for Configuration 5 36 in. Core - Row 11 Rods In

TABLE I. Number of Assemblies per Region for 40 in. Cores

Configuration	Ref	1	2	3	4	5	6	7	8	9	10	11	12a, 12b, 12c
Power, MWt	3300	3300	3300	3246	3246	3084	3084	3084	3084	3084	3084	3084	3084
Fuel Assemblies													
Core 1	48	48	48	48	48	48	36	36	36	36	36	36	36
Core 2	108	108	96	90	90	90	72	72	72	72	72	72	72
Core 3	210	210	222	222	222	204	234	234	234	234	234	234	222
Total	366	366	366	360	360	342	342	342	342	342	342	342	330
Internal Blanket Assemblies													
Internal Blanket 1	19	19	19	19	19	19	13	19	19	19	19	19	19
Internal Blanket 2	48	36	36	30	30	30	30	24	24	24	24	24	24
Internal Blanket 3	114	126	102	114	96	36	90	90	90	102	90	78	78
Internal Blanket 4	-	-	-	-	-	-	-	-	-	-	12	24	36
Total	181	181	157	163	145	145	133	133	133	145	145	145	157

TABLE II. Number of Assemblies per Region for 36 in. Cores

Configuration	Ref	1	2	3	4	5	5'[a]
Power, MWt	3300	3300	3300	3300	3300	3300	3300
Fuel Assemblies							
Core 1	72	48	60	48	48	48	48
Core 2	108	84	96	96	84	84	84
Core 3	174	222	198	210	222	210	210
Total	354	354	354	354	354	342	342
Internal Blanket Assemblies							
Internal Blanket 1	55	19	19	37	37	37	37
Internal Blanket 2	68	36	36	30	30	30	30
Internal Blanket 3	66	54	72	66	78	78	78
Total	169	109	127	133	145	145	145

[a]Case 5' uses the same configuration as case 5, but the core is 42 in. tall with 271 0.27 in. o.d. pins per assembly.

TABLE III. Inventory for 40 in. Cores

Configuration	Ref	1	2	3	4	5	6	7	8	9	10	11	12a, 12b, 12c
Power, MWt	3300	3300	3300	3246	3246	3084	3084	3084	3084	3084	3084	3084	3084
Specific Inventory, kg/MWt	1.43	1.42	1.37	1.39	1.35	1.38	1.34	1.34	1.34	1.37	1.38	1.37	1.38
BOEC Fissile Inventory, kg													
Core	4097.5	4078	3930	3916.0	3807.9	3700.4	3591.8	3586.9	3579.1	3658.5	3683.8	3675.1	3705.8
Internal Blanket	210.3	205	191	190.6	180.2	176.0	169.1	163.2	166.1	173.9	177.1	183.6	197.3
Radial Blanket	340.9	342	342	341.7	339.4	326.9	321.2	335.3	326.4	326.8	322.0	305.0	310.0
Axial Blanket	59.8	61	63	61.3	63.4	58.8	60.4	60.5	60.6	59.0	58.5	58.3	55.3
Total	4708.5	4686	4526	4509.6	4390.9	4262.1	4143.5	4145.9	4132.2	4218.2	4241.4	4222.0	4268.4
EOEC Fissile Inventory, kg													
Core	3773.3	3757	3627	3610.9	3518.6	3415.0	3319.0	3316.2	3308.2	3375.3	3399.6	3397.3	3408.3
Internal Blanket	591.7	578	537	536.1	504.7	493.8	473.0	437.3	465.1	488.0	496.5	513.1	551.8
Radial Blanket	498.5	500	500	499.7	496.4	477.8	469.7	489.7	477.1	477.6	470.8	446.5	453.5
Axial Blanket	174.6	176	184	178.7	184.8	171.6	176.0	176.6	176.7	172.3	170.7	170.1	161.4
Total	5038.1	5011	4848	4825.4	4704.5	4558.2	4437.7	4439.8	4427.1	4513.2	4537.6	4527.0	4575.0
Fissile Gain, kg/Cycle													
Core	-324.2	-321	-303	-305.0	-289.3	-285.4	-272.8	-270.7	-270.9	-283.2	-284.2	-277.8	-297.5
Internal Blanket	381.4	373	346	345.5	324.5	317.0	303.9	294.1	299.0	314.1	319.4	329.5	354.5
Radial Blanket	157.6	158	158	158.0	157.0	150.9	148.5	154.4	150.7	150.8	148.8	141.5	143.5
Axial Blanket	114.8	115	121	117.4	121.4	112.8	115.6	116.1	116.1	113.3	112.2	111.8	105.8
Net	329.6	325	322	315.8	313.6	296.1	295.2	293.9	294.9	295.0	296.2	305.1	306.6

TABLE IV. Inventories for 36 in. Cores

Congiguration	Ref	1	2	3	4	5	5'[a]
Power, MWt	3300	3465	3465	3300	3300	3300	3300
Specific Inventory, kg/MWt	1.33	1.27	1.30	1.21	1.27	1.27	1.37
EOEC Fissile Inventory, kg							
Core	3786.8	3596.1	3667.2	3443.0	3599.0	3585.8	3990.6
Internal Blanket	191.6	175.5	186.9	157.4	173.5	186.4	187.3
Radial Blanket	349.2	353.3	355.8	324.2	331.3	334.1	335.9
Axial Blanket	73.1	82.5	79.5	81.7	78.0	74.7	60.7
Total	4400.8	4207.3	4289.5	4006.3	4181.8	4181.0	4574.5
EOEC Fissile Inventory, kg							
Core	3456.5	3277.1	3336.5	3160.5	3294.7	3263.6	3708.3
Internal Blanket	538.1	488.8	521.8	436.8	483.7	520.7	525.8
Radial Blanket	510.7	515.8	519.3	474.5	484.4	488.5	491.8
Axial Blanket	212.9	239.1	230.9	236.8	226.5	216.9	177.4
Total	4718.2	4520.8	4608.5	4308.6	4489.3	4489.7	4902.9
Fissile Gain, kg/Cycle							
Core	-330.3	-319.0	-330.7	-282.5	-304.0	-322.2	-282.3
Internal Blanket	346.5	313.3	334.9	279.4	310.2	334.3	338.5
Radial Blanket	161.5	162.5	163.5	150.3	153.1	154.4	155.9
Axial Blanket	139.8	156.6	151.4	155.1	148.5	142.2	116.7
Net	319.6	313.5	319.0	302.3	307.6	308.8	328.5

[a]Case 5' uses the same configuration as case 5, but the core is 42 in. tall with 271 0.27 in. pins per assembly.

TABLE V. Burnup Parameters for 40 in. Cores

Configuration	Ref	1	2	3	4	5	6	7	8	9	10	11	12a 12b, 12c
Burnup Swing, %Δk	1.16	1.37	1.19	1.45	1.21	1.19	1.19	1.32	1.33	1.52	1.21	0.66	0.49
Burnup, MWD/kg Peak Discharge	82.6	83.6	83.9	85.2	84.3	82.0	82.6	85.0	84.1	83.1	85.4	83.5	83.8
Fast Fluence, 10^{23} nvt	1.41	1.45	1.45	1.46	1.48	1.44	1.42	1.42	1.42	1.40	1.43	1.44	1.44

TABLE VI. Burnup Parameters for 36 in. Cores

Configuration	Ref	1	2	3	4	5	5'[a]
Burnup Swing, % Δk	1.52	1.53	1.49	1.65	1.83	1.83	0.94
Burnup, MWD/kg Peak Discharge	83.3	91.5	88.1	85.8	86.7	92.9	80.4
Fast Fluence, 10^{23} nvt	1.47	1.65	1.59	1.52	1.50	1.63	1.47

[a]Case 5' uses the same configuration as case 5, but the core is 42 in. tall with 271 0.27 in. pins per assembly.

TABLE VII. Rating, Power Swings and Power Sensitivities to Enrichment Split Changes for 40 in. Cores

Configuration	Ref	1	2	3	4	5	6	7	8	9	10	11	12a, 12b, 12c
BOEC Rating, kW/ft													
Core 1	10.93	11.09	11.43	11.17	11.43	11.10	10.83	10.50	11.21	11.18	11.77	11.43	11.74
Core 2	11.69	11.25	11.49	11.68	11.83	11.54	11.15	11.86	11.66	11.21	11.95	12.07	11.59
Core 3	11.85	11.86	11.92	12.08	11.94	11.96	12.31	12.24	12.18	12.31	11.88	12.00	12.20
EOEC Rating, kW/ft													
Core 1	11.88	12.29	12.26	12.24	12.01	11.64	12.31	11.41	12.11	12.37	12.24	11.31	11.24
Core 2	11.67	11.90	11.88	12.31	12.04	11.70	12.05	12.18	12.18	12.31	12.21	11.60	11.54
Core 3	9.22	9.14	9.38	9.38	9.52	9.54	9.79	9.99	9.86	9.73	9.61	10.37	10.70
Rating Change, %													
Core 1	8.6	10.8	7.2	9.5	5.0	4.8	13.6	8.6	8.0	11.6	3.9	-1.0	-4.3
Core 2	0.2	5.7	3.3	5.3	1.7	1.3	7.4	2.6	4.4	9.8	2.1	-3.8	-0.4
Core 3	-22.1	-22.9	-21.3	-23.0	-20.2	-20.2	-20.4	-18.3	-19.0	-20.9	-19.1	-13.5	-12.3
Power Sensitivity Factor[a]	2.91	2.94	2.69	2.85	2.47	2.41	2.38	1.89	2.04	2.46	2.31	1.83	1.85

[a]% core 1 rating change due to 0.5% enrichment split change in that region.

TABLE VIII. Rating, Power Swings and Power Sensitivities to Enrichment Split Change for 36 in. Cores

Configuration	Ref.	1	2	3	4	5	5'[a]
BOEC Rating, kW/ft							
Core 1	10.8	11.0	11.2	11.1	11.0	11.9	12.6
Core 2	10.5	10.7	11.0	11.3	11.2	11.7	12.6
Core 3	10.5	10.8	10.9	11.5	11.5	10.7	11.7
EOEC Rating, kW/ft							
Core 1	9.9	10.5	11.0	10.7	10.9	11.1	12.2
Core 2	9.7	10.2	10.5	10.6	10.8	10.9	12.1
Core 3	9.2	9.0	9.3	9.8	9.6	9.2	10.1
Rating Change, %							
Core 1	-8.3	-4.5	-1.8	-3.6	-0.9	-6.7	-3.2
Core 2	-7.6	-4.7	-4.5	-6.2	-3.6	-6.8	-4.0
Core 3	-12.3	-17.7	-14.7	-14.8	-16.5	-14.0	-13.7
Power Sensitivity Factor[b]	2.52	2.74	2.05	1.49	1.76	1.95	

[a] Case 5' uses the same configurations as Case 5, but the core is 42 in. tall with 27 ft 0.27 in. pins per assembly.

[b] % Core 1 rating change due to 0.5% enrichment split change in that region.

TABLE IX. Breeding Performances and Sodium Void Reactivities for 40 in. Cores

Configuration	Ref	1	2	3	4	5	6	7	8	9	10	11	12a, 12b, 12c
BR	1.368	1.365	1.359	1.360	1.355	1.353	1.357	1.351	1.352	1.354	1.353	1.358	1.361
RDT	14.3	14.4	14.1	14.3	14.0	14.4	14.0	14.1	14.0	14.3	14.3	13.8	13.9
CSDT	16.3	16.4	16.1	16.3	15.9	16.4	15.9	16.1	15.9	16.3	16.3	15.6	15.7
EOEC Sodium Void Reactivity[a]													
%k	0.801	0.825	0.885	0.847	0.920	0.890	0.891	0.894	0.895	0.837	0.874	0.924	0.871
$	2.19	2.26	2.42	2.32	2.52	2.44	2.44	2.45	2.45	2.29	2.39	2.53	2.38

[a]For voiding flowing sodium in the core and upper axial blanket regions.

TABLE X. Breeding Performances and Sodium Void Reactivities for 36 in. Cores

Configuration	Ref.	1	2	3	4	5	5'[a]
BR	1.355	1.336	1.342	1.334	1.341	1.346	1.365
RDT	13.9	13.3	13.6	13.4	13.5	13.5	13.9
CDST	15.7	14.9	15.4	15.1	15.2	15.3	15.8
EOEC Sodium Void Reactivity[b]							
% Δk	0.826	0.979	0.921	0.905	0.830	0.807	0.930
$	2.28	2.71	2.55	2.50	2.29	2.23	2.57

[a]Case 5' uses the same configuration as case 5, but the core is 42 in. tall with 271 0.27 in. pins per assembly.

[b]For voiding flowing sodium in the core and upper axial blanket regions.

TABLE XI. Peak-to-Average Ratings for 40 in. Core With 12a, 12b and 12c Core Configuration (HEX Calculations)

	BOL	BOEC	MOEC	EOEC
12a				
Core 1	1.357	1.357	1.356	1.356
Core 2	1.407	1.390	1.375	1.362
Core 3	1.539	1.512	1.545	1.604
12b				
Core 1	1.372	1.372	1.373	1.373
Core 2	1.339	1.331	1.323	1.316
Core 3	1.552	1.522	1.537	1.594
12c				
Core 1	1.362	1.361	1.364	1.364
Core 2	1.342	1.337	1.327	1.321
Core 3	1.495	1.489	1.480	1.581

TABLE XII. Peak Ratings (kW/ft) for 40 in. Cores With 12a, 12b and 12C Core Configurations (HEX Calculations)

	BOL	BOEC	MOEC	EOEC
12a				
Core 1	12.74	11.76	11.27	10.71
Core 2	13.88	12.79	12.25	11.61
Core 3	13.76	12.81	12.50	12.54
12b				
Core 1	13.27	12.30	11.71	11.10
Core 2	13.70	12.72	12.15	11.56
Core 3	13.26	12.52	12.26	12.31
12c				
Core 1	13.15	12.31	11.51	11.06
Core 2	13.39	12.56	11.83	11.40
Core 3	13.26	12.41	11.96	12.28

TABLE XIII. Control Rod Worths for 40 in. Cores With 12a, 12b and 12c Core Configurations

	Configuration		
	12a	12b	12c
Primary system			
Location	Row 7 Row 11	Row 7 Row 11	Row 7 Row 11
Worth % Δk	4.25	4.47	4.65
$	11.64	12.25	12.74
Secondary system			
Location	Row 5 Row 13	Row 4 Row 13	Row 4 Row 13
Worth, % Δk	3.71	3.34	3.26
$	10.16	9.15	8.93

APPENDIX E: COMPONENT DESIGN

Table of Contents

		Page
1.0	INTRODUCTION	E-1
2.0	COMPONENT DESIGN CONSIDERATIONS	E-3
2.1	General Features of Pool Type PLBR's	E-3
2.2	Reactor Support Grid Sleeves and Fuel Assembly Discriminator Features	E-4
2.3	Fuel Assembly Spacing Devices	E-6
2.4	Fuel Assembly Outlet Mixing Devices	E-6
2.5	Fuel Assembly Duct Wall Thickness Reduction	E-7
2.6	Fuel Assembly Upper Adapter Holddown	E-8
2.7	Fuel Assembly Preliminary Layout	E-9
2.8	Control Rod Preliminary Layout	E-9

List of Figures

No.	Title	Page
1.	Reactor-support-grid Sleeves and Discriminator Scheme	E-10
2.	Fuel Assembly Lower Adapter with Discriminator Keys	E-11
3.	Fuel Assembly Spacing Device	E-12
4.	Fuel Assembly Outlet Mixing Device	E-13
5.	Fuel Assembly Duct Flow Restrictors	E-14
6.	Fuel Assembly Upper Adapter Flow Restrictor	E-15
7.	Fuel Assembly Upper Adapter Holddown Scheme	E-16
8.	Fuel Assembly Preliminary Layouts	E-17
9.	Control Rod Preliminary Layout	E-18

APPENDIX E: COMPONENT DESIGN

by

E. Hutter and R. V. Batch

1.0 INTRODUCTION

Because of the preliminary nature of the PLBR Core Design optimization work presented in this series of reports, the component design activity, at this stage, deals primarily with generic options of various design aspects. The major areas of effort cover the following items:

- GENERAL FEATURES OF POOL TYPE PLBR's.
- REACTOR SUPPORT GRID SLEEVES, AND FUEL ASSEMBLY* DISCRIMINATOR FEATURES.
- FUEL ASSEMBLY SPACING DEVICES.
- FUEL ASSEMBLY OUTLET MIXING DEVICES.
- FUEL ASSEMBLY DUCT WALL THICKNESS REDUCTION.
- FUEL ASSEMBLY UPPER ADAPTER HOLDDOWN.
- FUEL ASSEMBLY PRELIMINARY LAYOUT.
- CONTROL ROD PRELIMINARY LAYOUT.

*In most parts of this text, the term "fuel assembly" also applies to blanket assemblies, reflector assemblies, shield assemblies, etc.

2.0 COMPONENT DESIGN CONSIDERATIONS

2.1 GENERAL FEATURES OF POOL TYPE PLBR'S

Consultations were held with W. Barthold, et al., concerning overall reactor aspects such as size, height, configuration, etc., and their impact on other systems, primarily fuel loading, sodium-pool tank size, rotating plug dimensions, etc.

Reactor vessel diameter size depends on:

- Core, reflector, and blanket diameters.
- Thickness of shielding inside the reactor vessel.

The reactor vessel diameter affects:

- Rotating shield plug size, (depending on the size of the area needing fuel assembly insertions and removals).
- Instrument tree size and spread, including possible steadying bars and their sweep during plug rotation.
- The type of In-Vessel-Handling Machine (IVHM), such as straight pull, fixed offset, pantagraph, etc.
- The location of the ex-reactor vessel fuel assembly transfer point, for tilted entrance and exit ramps, and the angle of these ramps.
- The sodium-pool and tank diameter. Excessive rotating shield plug size affects the spacing circle of the pumps and heat exchangers which in turn increases the diameter of the sodium-pool tank. However a very small rotating shield plug, although very desirable for fabrication and economic reasons, does not reduce the primary tank diameter below the minimum dictated by the number and by the size of the primary system pump and IHX plugs.

The fuel assembly length depends on:

- The core and blanket lengths.
- The length of the gas space.

- The lengths of the top and bottom adapters.
- The space needed for transition sections, element support grids, coolant mixing devices, etc.

The fuel assembly length affects:

- Sodium-pool tank depth, that in turn affects the amount of sodium, weight, support, seismic behavior, etc. of the tank. Any increase to the fuel assembly length adds twice that dimension to the depth of the tank. (Because of in-sodium fuel handling requirements.)
- IVHM, because any increase of the fuel assembly lengths adds once or twice that dimension to the overall length of the IVHM and to other fuel handling devices.

Previous studies (ANL-76-61, An Overview of Pool-type LMFBR's by A. Amorosi, E. Hutter, et al., Chapters V and VI) describe various fuel handling methods and primary-system configurations and options. Assuming that a straight push-pull IVHM is used, in conjunction with a double or triple rotating shield plug, and a tilted entrance and exit ramp, a reactor of approximately 16 ft. diameter requires a 30 ft. diameter large-rotating-shield plug. A rotating plug of this magnitude seems to approach the maximum size and weight for such a component, that could be provided without exorbitant cost penalties. Similarly, a 15-16 ft. overall length for fuel assemblies represents an acceptable design, although any reduction of these dimensions is very desirable.

2.2 REACTOR SUPPORT GRID SLEEVES AND FUEL ASSEMBLY DISCRIMINATOR FEATURES

The purposes of replaceable sleeves are:

- Reactor support grid protection.
- Relatively easy removal of the fuel assembly seats from the reactor support grid.
- Possibility of changing the support grid pattern during the reactor life time.
- Easier and cheaper fabrication of the reactor support grid. The additional cost of the sleeves may nullify any savings, however, fabrication errors would in many instances by of lesser consequences.
- Providing filtering devices (which may or may not be desirable).

The purposes of reactor support grid keys are:

- Primarily to prevent insertion of fuel assembly into the wrong reactor region.
- To confirm fuel assembly orientation within 180°. (This may not apply to commercial breeders).
- To provide a reasonable number (<15) of easily discernable zones.

The different shapes and diameters of the fuel assembly bottom adapters and their corresponding receptables and orientation bars must be dimensionally distinct enough, so as to eliminate any possibility of jamming a bottom adapter into the wrong opening. Therefore nominal "horizontal" dimensions should vary by 0.200 in. or more, and the "vertical" dimensions (points of interference) should provide 6 in. or more for distinction.

The enclosed illustrations (Figs. 1 and 2) show a concept of individual sleeves and of a simple discriminator scheme.

The main features are:

- Each sleeve can be individually inserted or removed from the reactor support grid.
- Each sleeve is fastened to the reactor support grid by a bayonet lock (no movable parts).
- Each sleeve is prevented from rotating (loosening) during reactor operation, by the inserted fuel assembly lower adapter.
- Each sleeve provides distinct grooves for the discriminator keys of the fuel assembly lower adapter.
- Each fuel assembly lower adapter has 2 keys (orientation and discrimination) of different width, mounted at different elevations.
- The orientation key is narrower and engages first. It ascertains that the fuel assembly faces in the right direction, and is not oriented wrongly in multiples of 60°.
- If a 180° rotation during a fuel assembly life time is desirable, a second orientation key groove may be provided in the sleeve.
- The discrimination key is wider. For each zone, it is mounted at a different angle (e.g., 45° increments) from the orientation key.

- Except for the orientation of the discrimination key, all other outer diameters of the lower adapters remain the same. This simplifies fabrication and lowers the inventory.

2.3 FUEL ASSEMBLY SPACING DEVICES

The main purposes of fuel assembly spacing devices are:

- To provide uniform spacing between the hexagonal ducts to minimize the effects of leaning, bowing, creeping, bulging, etc.
- To reduce seismic effects.
- To ease fuel handling.

There is a variety of fuel assembly spacing devices. However, one should distinguish between spacers and devices that also act as seals of the gaps between the hexagonal ducts. The real spacers could be made of solid metal napkin-ring type bands, that would contact their counterparts at predetermined elevations. However, the solid metal and/or the circumferential contact may cause excessive friction.

The enclosed illustration (Fig. 3) shows a concept that minimizes the undesirable points.

Its main features are:

- Metal-to-metal contact is only made near the corners of the hexagonal duct.
- Clearance is left near the center portion of the hexagonal duct flat, where bulging is most likely to occur.
- The spacer may be made as a napkin-ring to be fastened at various elevations, or it may be part of the upper adapter.

2.4 FUEL ASSEMBLY OUTLET MIXING DEVICES

The main purpose of fuel assembly outlet mixing devices are:

- To reduce the magnitude of thermal striping of sodium in the space above the fuel assemblies.
- To reduce the thermal stress on various permanent or semi-permanent "upper internals" caused by temperature differences of the effluent coolant from adjacent fuel assemblies.

The enclosed illustration (Fig. 4) shows a concept that has the following features:

- Mixing is accomplished by directing part of the effluent coolant sideways, so that it can readily interact with the effluents from the neighboring fuel assemblies.
- The mixing device has no moving parts and is not exposed to significant temperature changes during steady-state reactor operation.
- The mixing device is part of the fuel assembly and is therefore removed with each fuel assembly loading.

2.5 FUEL ASSEMBLY DUCT WALL THICKNESS REDUCTION

The main reasons for reducing the duct wall thickness (from about 0.150 in. to about 0.040 in.) are:

- The decreased mass of structural material increases the fuel volume fraction and may decrease the reactor diameter.
- The decreased mass of structural material also decreases the parasitic neutron absorptions and thus improves breeding performance.
- Hexagonal ducts with heavy walls are more costly than those with thinner walls (within limits).

To a large extent, the hexagonal duct wall thickness is determined by the pressure differential between the inside and the outside of the duct. Reduction of this pressure differential would make it possible to make the duct wall thinner. The internal pressure is determined by the fuel assembly pressure drop caused by the required coolant flow velocity and no significant reduction can be counted on. Therefore the attempt has to be made to raise the pressure on the outside of the duct wall. This in turn would substantially increase the bypass flow unless flow-restrictors or seals are provided across the approximately 0.150 in. wide gap between the hexagonal ducts.

The enclosed illustrations (Figs. 5 and 6) show several concepts that have the following features:

- The flow restrictors are part of each fuel assembly, and are therefore removable and their life time is relatively short.

- The flow restrictors have some flexibility, to accommodate the shifting of ducts due to thermal effects, the bulging of ducts due to creep, etc.
- The flow restrictors shown on Fig. 5 can be located at any desirable elevation.
- The flow restrictors do not pose any problems in fuel handling.
- The flow restrictors are not likely to be accidentally damaged or ripped off.

2.6 FUEL ASSEMBLY UPPER ADAPTER HOLDDOWN

While deliberating some of the aforegoing topics, various answers to related aspects were attempted. One of these is the combination of duct-gap flow restrictors with a back-up mechanical holddown device.

The reasons for such a scheme would be:

- Although fuel assembly hydraulic holddown features are contemplated, it may be prudent to provide (if possible) a backup mechanical holddown device.
- Reasons for duct-gap restrictors are given in item 5.

The enclosed illustration (Fig. 7) shows a concept that has the following features:

- A stiff, but somewhat flexible beloows arrangement becomes a part of each fuel assembly upper adapter end.
- Each bellows has a seal ring at its free upper end which matches with a round opening of a perforated depressor plate.
- The depressor plate is part of the instrument tree and stretches across the entire reactor to the reactor barrel.
- During reactor operation, the depressor plate rests on the fuel assembly bellows seal rings and on the reactor barrel peripheral seal, compressing them slightly.
- Each bellows has enough compression space left to allow for thermal or radiation induced growth of the fuel assembly.
- The depressor plate may have some fuel assembly locating devices that extend below its soffit.

- The depressor plate also connects to coolant outlet mixing devices that help to support coolant monitoring instrument leads.
- The mixing devices are part of the semi-permanent instrument tree, which is less desirable than having mixing devices as part of each fuel assembly.

2.7 FUEL ASSEMBLY PRELIMINARY LAYOUT

The enclosed illustration (Fig. 8) shows 2 preliminary concepts of a fuel assembly, incorporating many of the ideas described above. The major difference between the 2 concepts is that one utilizes a reactor support grid sleeve that extends upward beyond the reactor support grid to an elevation near the bottom of the reactor core. This gives the fuel assembly a fixed support at a higher elevation than the companion scheme and thus may reduce the effect of tilting and bowing. However, because all portions of the sleeve have to be cylindrical, the lower portion (below the core) of all fuel assemblies would have to differ in design from the upper portions. The scheme with the short sleeve employs fuel elements virtually extending along the full length of the hexagonal duct, each fuel element containing not only the fuel but also the blanket material and the gas expansion chamber.

2.8 CONTROL ROD PRELIMINARY LAYOUT

The enclosed illustration (Fig. 9) shows a preliminary concept of a control rod and a control rod thimble allowing 40 in. vertical movement.

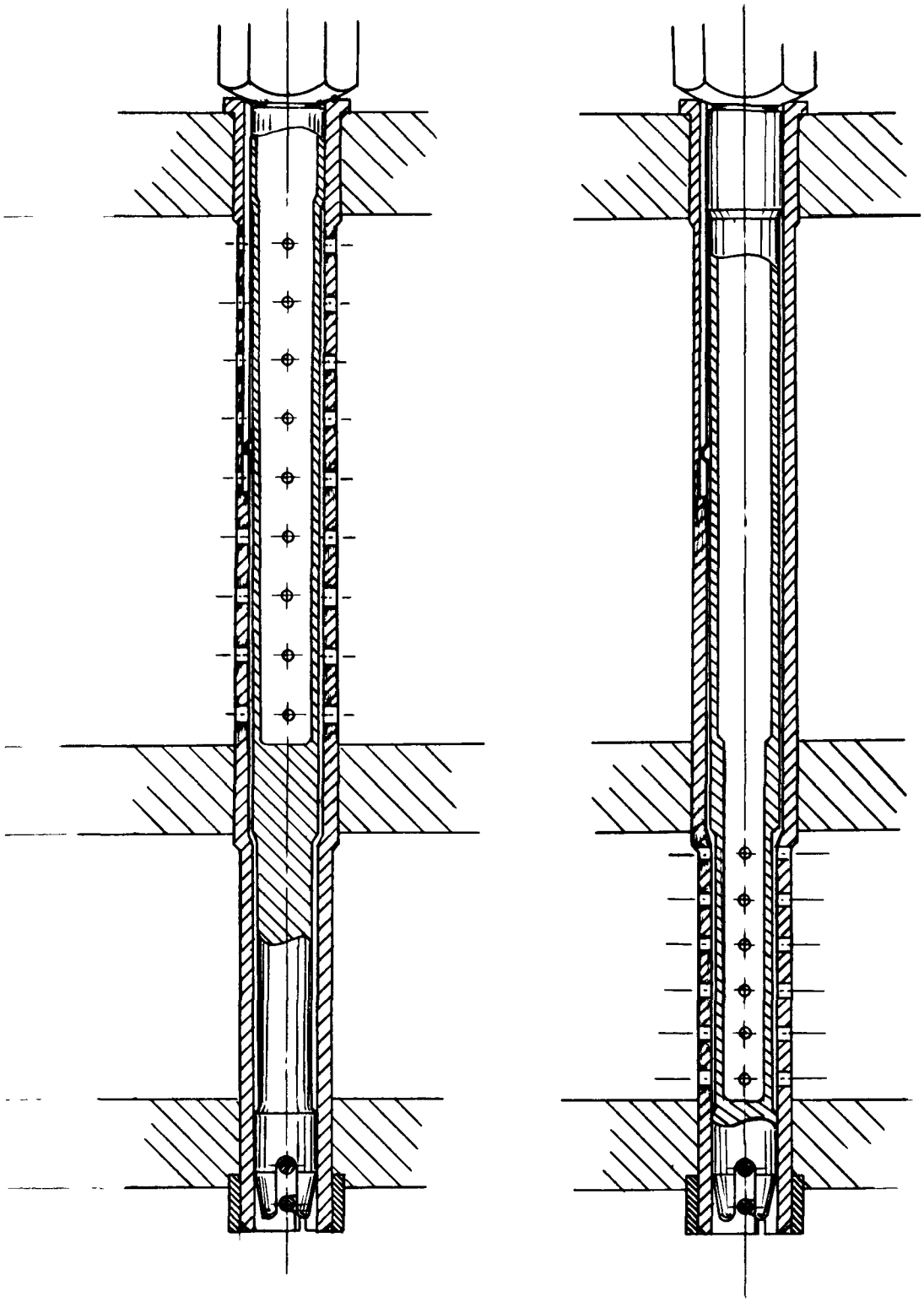

Fig. 1. Reactor-support-grid Sleeves and Discriminator Scheme

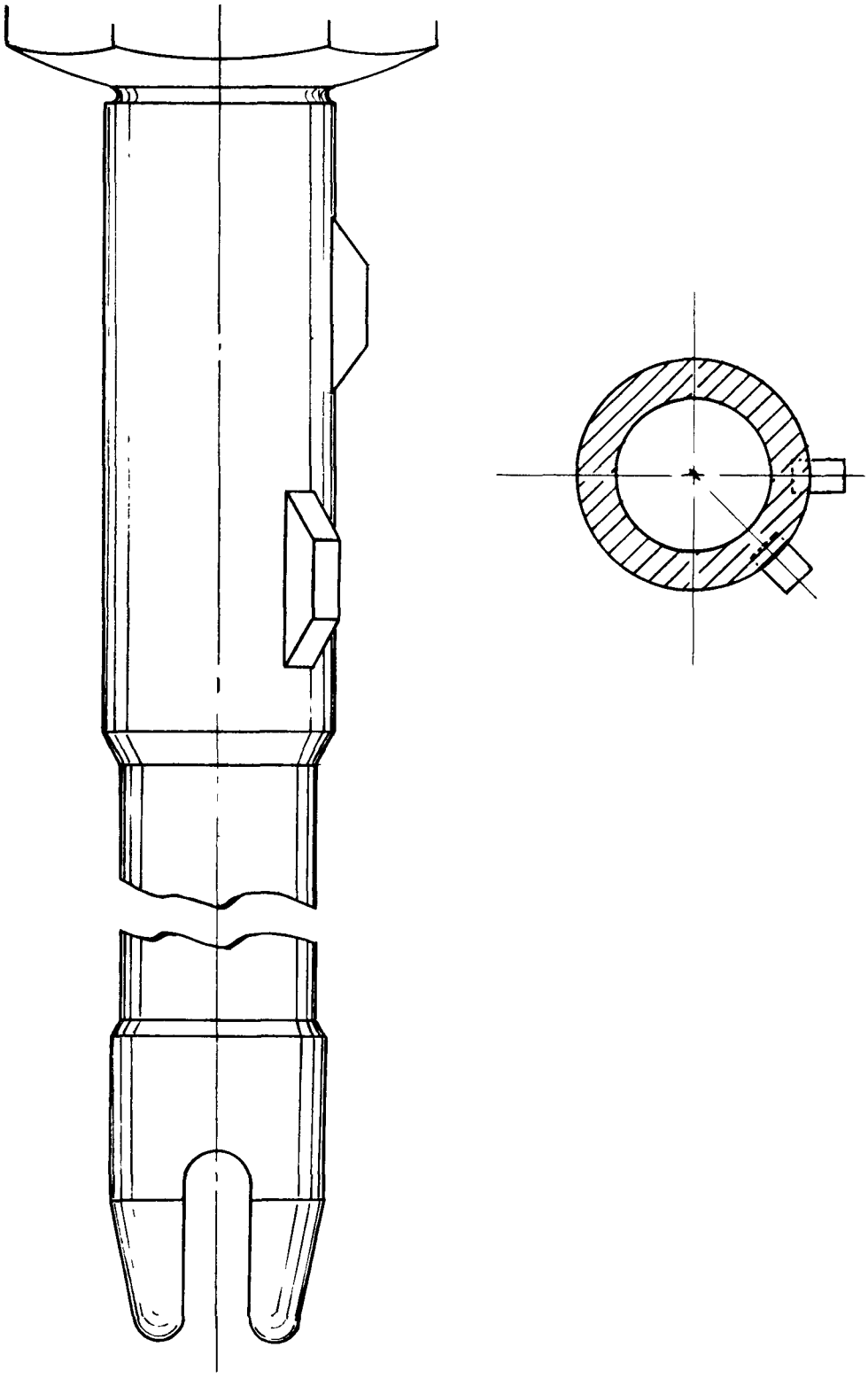

Fig. 2. Fuel Assembly Lower Adapter with Discriminator Keys

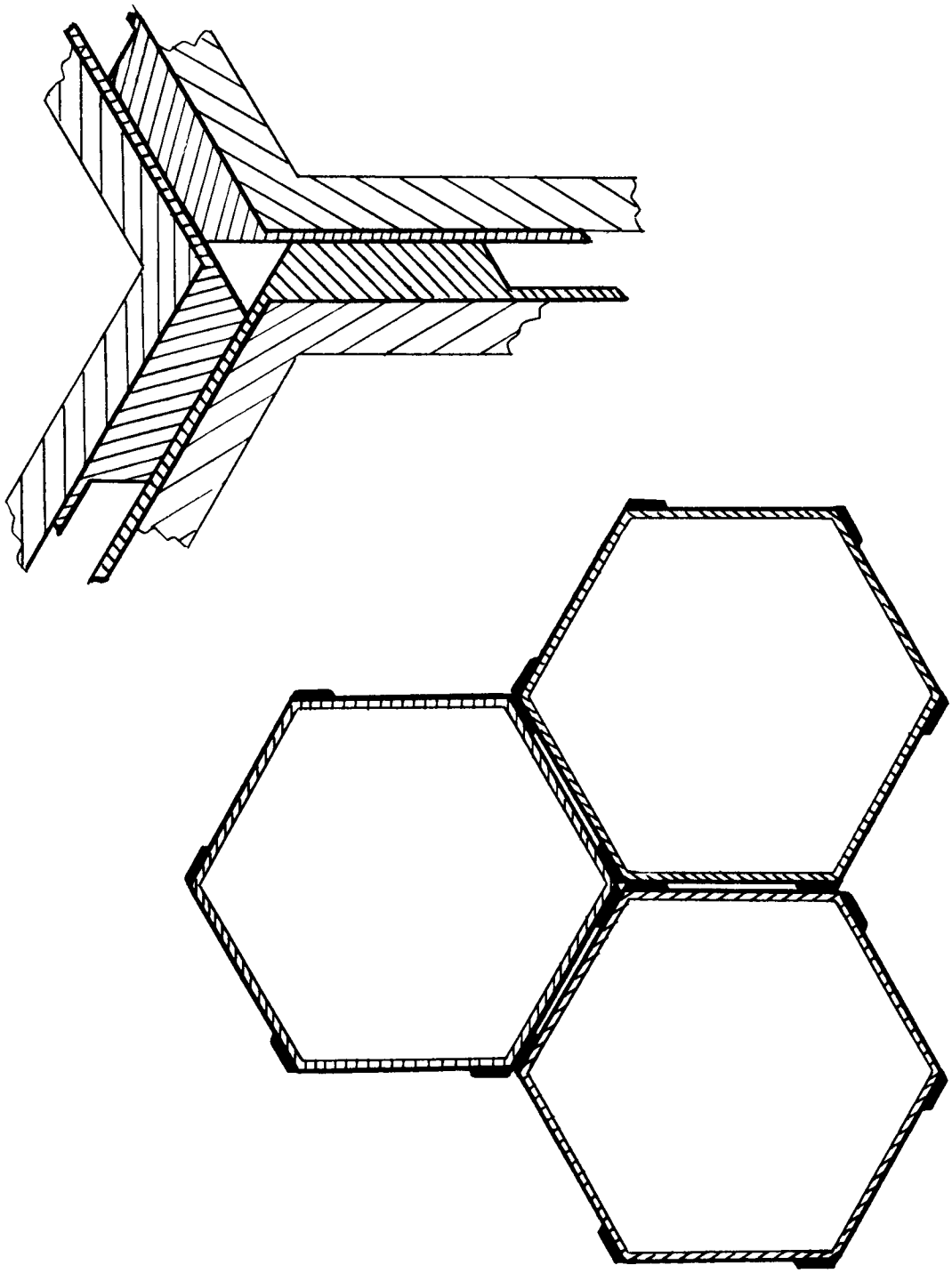

Fig. 3. Fuel Assembly Spacing Device

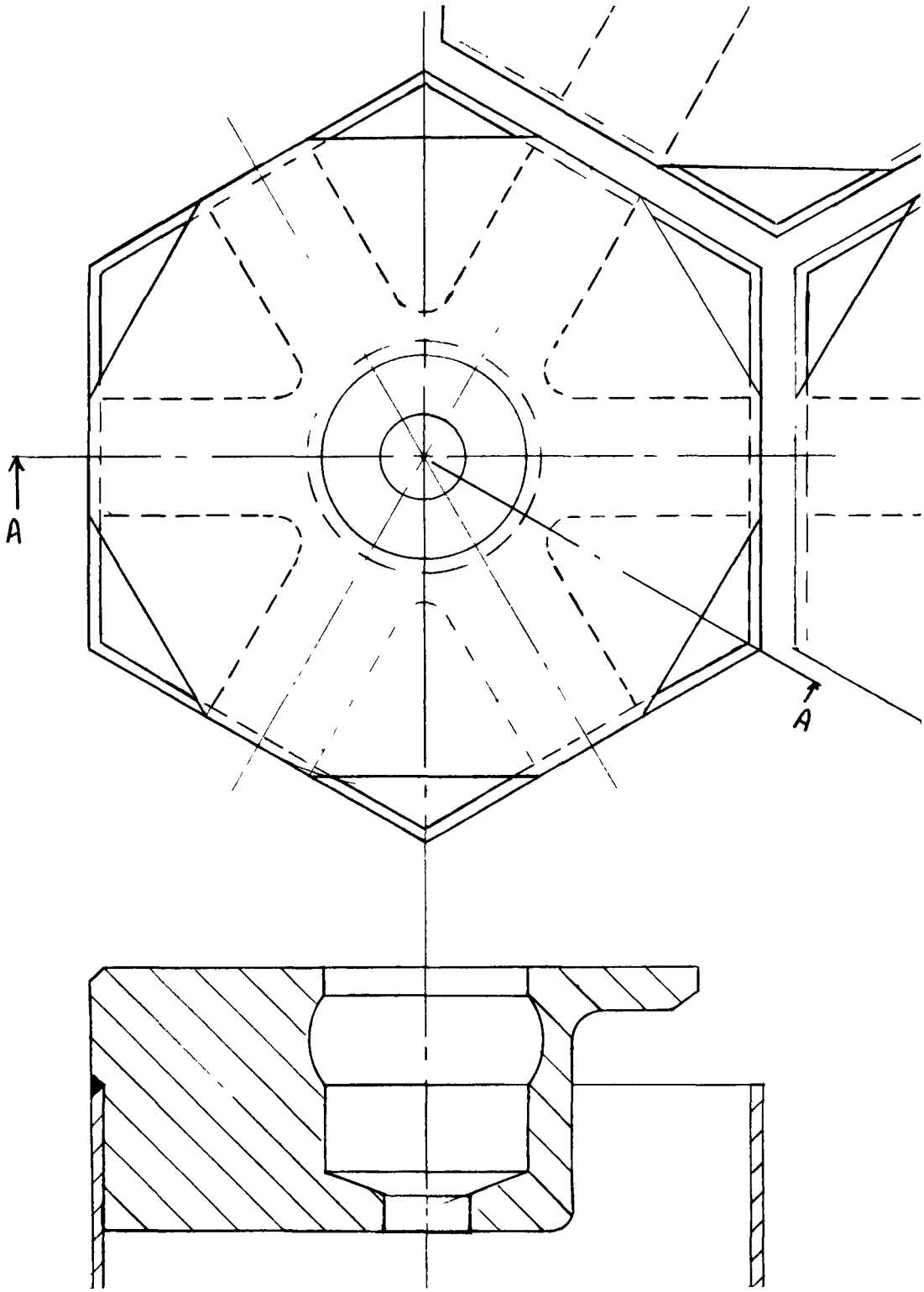

Fig. 4. Fuel Assembly Outlet Mixing Device

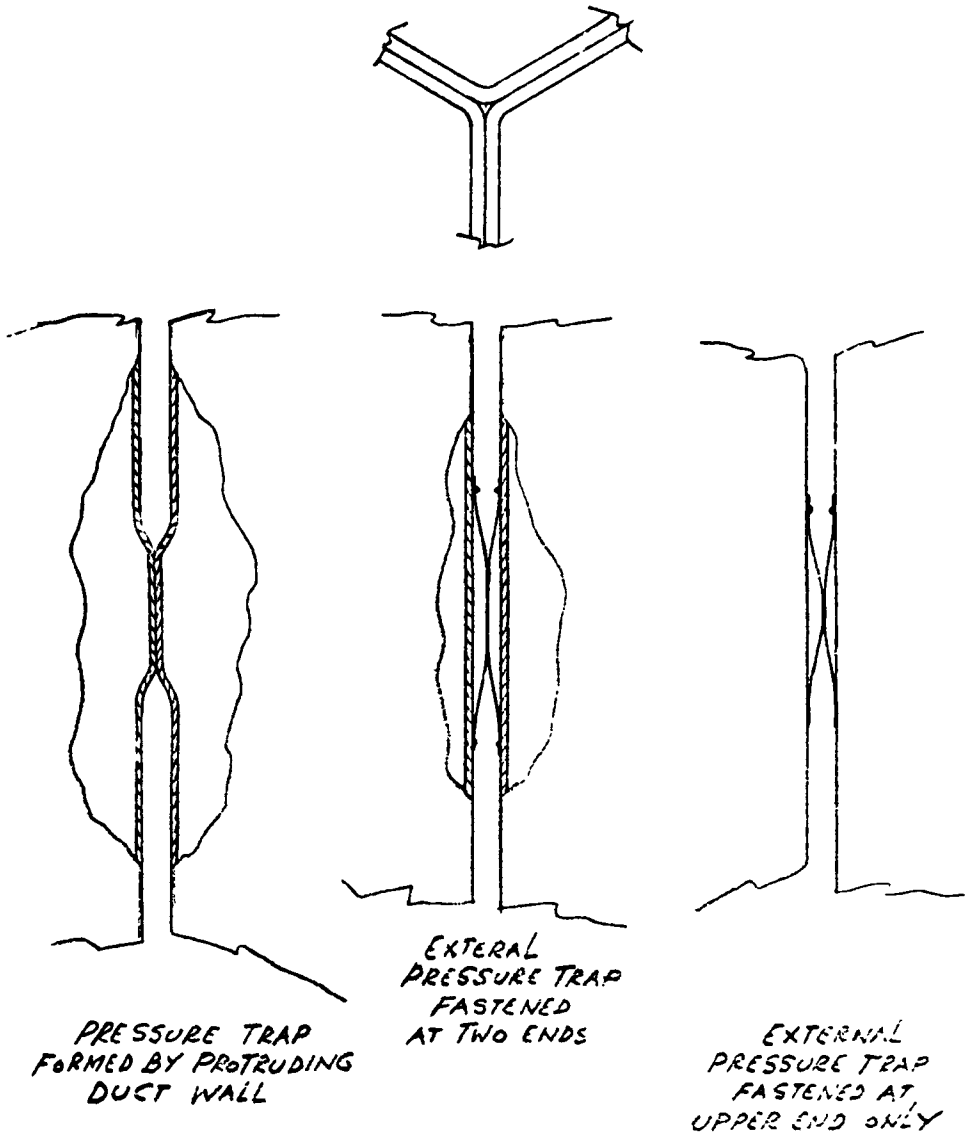

Fig. 5. Fuel Assembly Duct Flow Restrictors

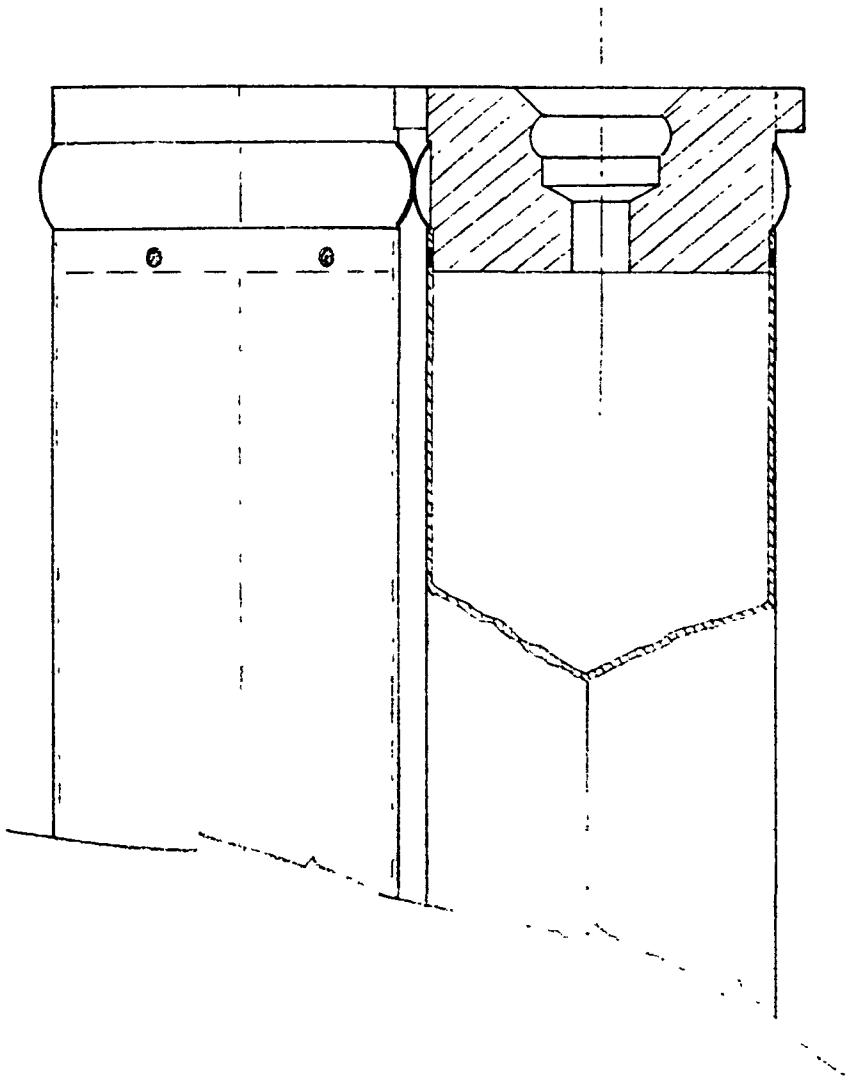

Fig. 6. Fuel Assembly Upper Adapter Flow Restrictor

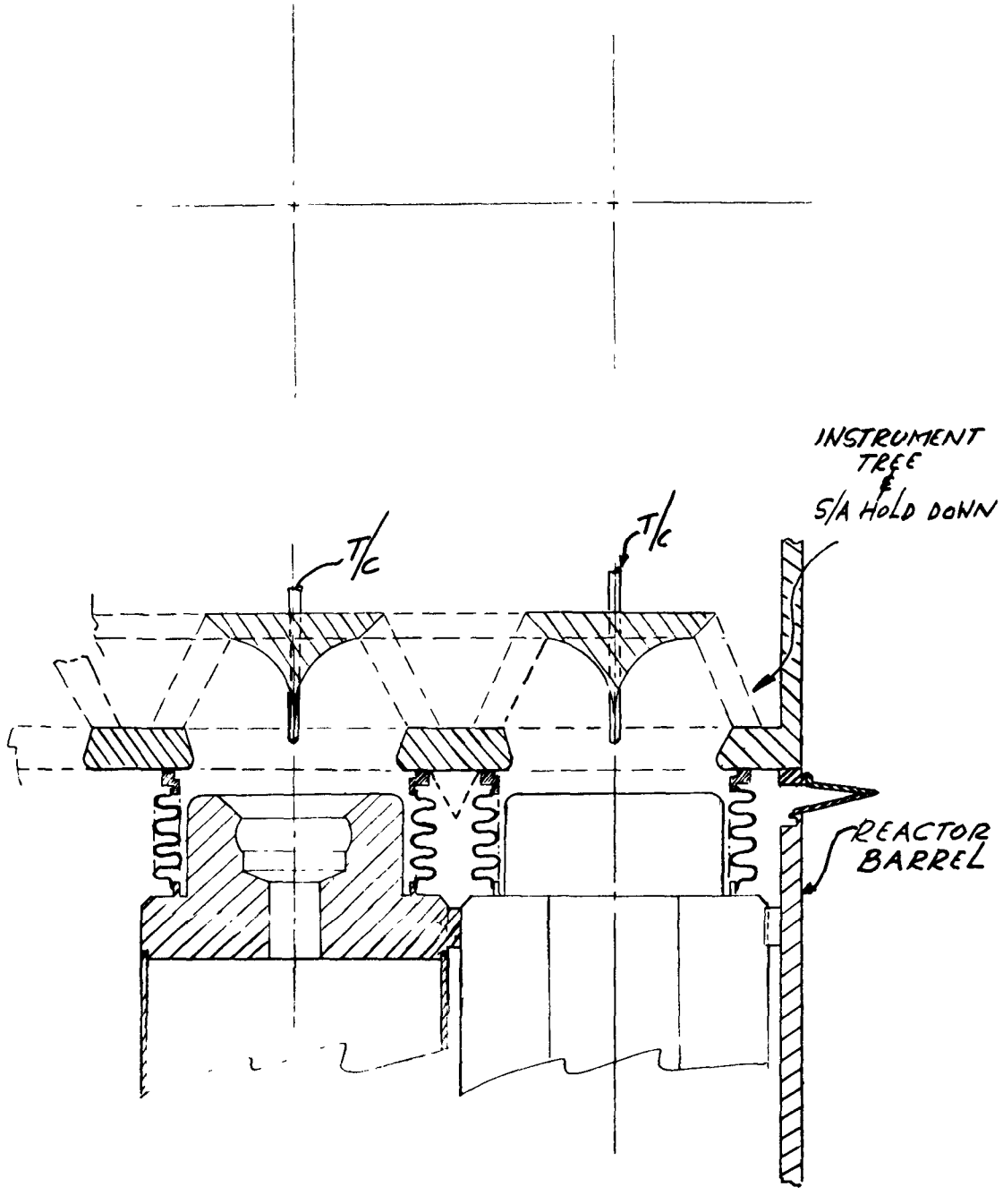

Fig. 7. Fuel Assembly Upper Adapter Holddown Scheme

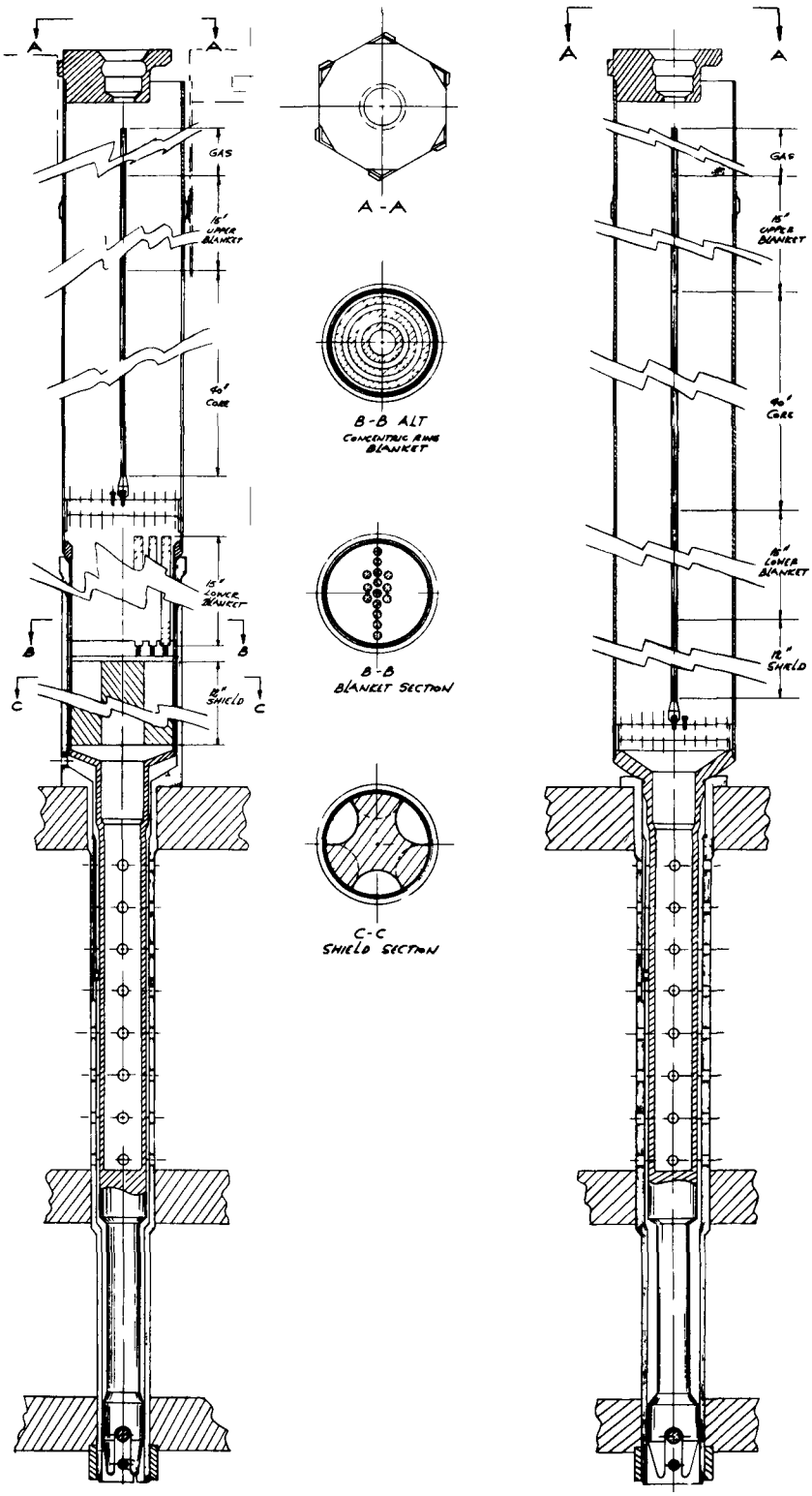

Fig. 8. Fuel Assembly Preliminary Layouts

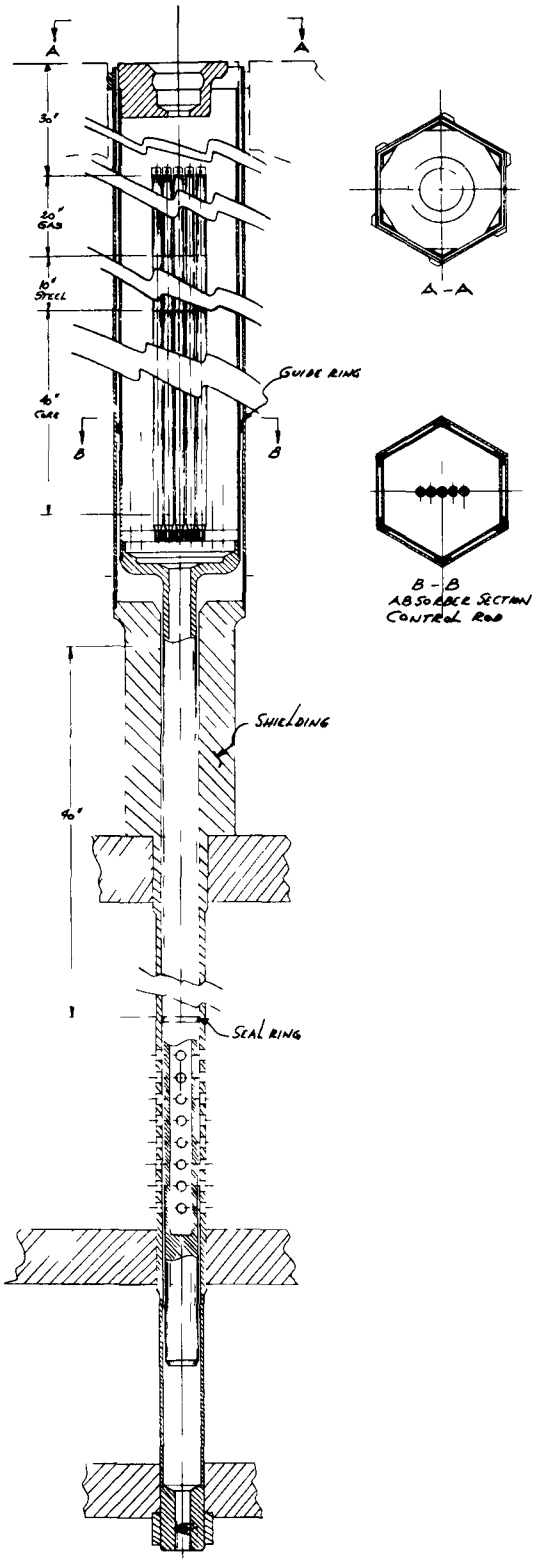

Fig. 9. Control Rod Preliminary Layout